

## A novel statistical performance evaluation of most modern optimization-based global MPPT techniques for partially shaded PV system



Hegazy Rezk<sup>a,b,\*</sup>, Mazen AL-Oran<sup>c</sup>, Mohamed R. Goma<sup>c,d</sup>, Mohamed A. Tolba<sup>e</sup>, Ahmed Fathy<sup>f,g</sup>,  
 Mohammad Ali Abdelkareem<sup>h,i,j</sup>, A.G. Olabi<sup>h,i,k,\*\*</sup>, Abou Hashema M. El-Sayed<sup>b</sup>

<sup>a</sup> College of Engineering at Wadi Addawaser, Prince Sattam Bin Abdulaziz University, Saudi Arabia

<sup>b</sup> Electrical Engineering Department, Faculty of Engineering, Minia University, Egypt

<sup>c</sup> Mechanical Department, Faculty of Engineering, Mu'tah University, Al-Karak, Jordan

<sup>d</sup> Mechanical Department, Benha Faculty of Engineering, Benha University, Benha, Egypt

<sup>e</sup> Nuclear Researches Center, Egyptian Atomic Energy Authority, Cairo, Egypt

<sup>f</sup> Electrical Engineering Department, Faculty of Engineering, Jouf University, Sakaka, Saudi Arabia

<sup>g</sup> Electrical Power and Machine Department, Faculty of Engineering, Zagazig University, Egypt

<sup>h</sup> Dept. of Sustainable and Renewable Energy Engineering, University of Sharjah, P.O. Box 27272, Sharjah, United Arab Emirates

<sup>i</sup> Center for Advanced Materials Research, University of Sharjah, PO Box 27272, Sharjah, United Arab Emirates

<sup>j</sup> Chemical Engineering Department, Faculty of Engineering, Minia University, Egypt

<sup>k</sup> Mechanical Engineering and Design, Aston University, School of Engineering and Applied Science, Aston Triangle, Birmingham, B4 7ET, UK

### ARTICLE INFO

#### Keywords:

Modern optimization approaches

MPPT

PV system

Partial shading

Energy efficiency

### ABSTRACT

A novel statistical performance evaluation of most modern optimization-based global MPPT techniques for partially shaded PV system is presented in this paper. In recent years, there has been a growing attention toward mitigation of partial shading effect of the PV system through using modern optimization. The field of tracking MPP of the PV system attracts huge attention from the researchers, as it is the best way to increase PV plant efficiency. Under non-uniform solar irradiance, the power against voltage characteristics of PV array have more than one MPP. This condition leads to extra complications to track MPP and decreases the efficiency of the PV system. Traditional MPPT methods are typically used to increase the harvested energy of PV under normal conditions without any problems. The key drawback of such methods is failing extraction of global MPP under actual weather conditions that sometimes under shadowing condition. Several global MPPT methods based on modern optimization are presented for extracting global MPP in case of shadowing condition. The essential target of this work is not limited to present an integrated specific review on the state-of-the-art of these techniques; but also a comprehensive statistical evaluation of twenty optimizers that represent high percent of all the reported techniques is performed with changing shading scenarios. This work serves as a source of valuable information for researchers and engineers working with PV systems to keep abreast with the modern advance in the field of tracking MPP of PV system.

### 1. Introduction

The rapid growth of population, industry and technological progress have led to an ever-increasing human need for energy. Energy is an important factor that plays a master role in the growth and development of technology, economic and existence life of the human around the world regions. Generally, a sharp increase for energy requirements for electrical consumption demand located on a rapid increase in the human population number [1–4]. The amount of energy consumption

in the developed country raises annually on an average of 1% and 5% [5]. The large portion of generated electricity is coming from utilizing fossil fuels such as coal, natural gas, and oil [6,7]. In fact, rapid increase of utilized fossil fuels and limited production of this fuel in a huge number of countries around the world lead to large depletion of fossil fuel and increase the level of price causing environment issues such as acid rain, air pollution and global warming [8,9]. Currently, the electrical generation through renewable energy practically solar energy became the most popular and promising technology option to minimize

\* Corresponding author. College of Engineering at Wadi Addawaser, Prince Sattam Bin Abdulaziz University, Saudi Arabia.

\*\* Corresponding author. Dept. of Sustainable and Renewable Energy Engineering, University of Sharjah, P.O. Box 27272, Sharjah, United Arab Emirates.

E-mail addresses: [hegazy.hussien@mu.edu.eg](mailto:hegazy.hussien@mu.edu.eg) (H. Rezk), [aolabi@sharjah.ac.ae](mailto:aolabi@sharjah.ac.ae) (A.G. Olabi).

the dependence on traditional energy source [10,11]. PV system can be employed to overcome the mentioned issues by converting solar irradiance directly to electricity [12,13]. PV stands out as one of the greatest technological developments [14,15]. Nowadays, it has achieved more distinctive attention than other types of renewable energy sources (RESs) due to its wide applications. In comparison with traditional power generation systems, PV has enormous advantages such as reliable system, low cost of operation and maintenance, free energy source, noise-free [16], clean and high availability source [17], and it does not cause any environment problem or emissions of toxic gases [18]. On the other hand, the massive area required for installation, cell degradation, low power efficiency, lower conversion from light to electricity under weak radiation condition are the large-scale limitations facing the PV systems [19]. PV system has been utilized in many applications like water pumping [20,21], moving carriers [22], batteries, remote or mobile storage of medicines and vaccines, consumer products such as watches, calculators, and radio. Also, it can be used in the streetlight, the lighting of the remote sign, and scientific research at temporary sites far from the conventional power source, building integrated photovoltaic systems (BIPV), water desalination and other applications that required electricity.

To increase PV system efficiency, maximum power point tracking (MPPT) algorithm is essential for harvesting maximum power from the PV system [23–25]. The MPPT which a key element in the PV system [26,27] is based on moving the operating PV voltage, or current, in order to get the maximum power [28]. The output power of PV system is dependent on environment conditions like temperature [29], solar irradiance level [30], shading, load [31], thermal characteristics [32] and dust accumulation [33,34]. Such parameters may decrease the efficiency of the PV system [35,36]. Therefore, they must be controlled and taken under consideration to maximize the power output of the PV system [37,38].

Partial shading condition (PSC) due to nearby trees, buildings, birds, or bird litters is an important issue associated with PV system performance [39]. In general, the shadow may be fully or partially according to the percentage of area that shades the PV module [40]. It directly affects both the cell temperature and irradiance level incident on the PV system [41]. Fully or partially, the shadow is considered as the major factor that reduces the harvested energy from the PV system [42]. Under shading condition, several maximum power points will appear on the curve of power against voltage resulting in more complicated characteristic [43,44]. Mitigation of partial shading condition (PSC) can be achieved by many approaches. These approaches include, installing the module of PV array on an area far away from building and trees and other factors that prevent the solar irradiation from reaching the total area of the module, connecting bypass diodes in parallel with each PV panel to avoid hotspot problem [45,46]. The MPPT methods are used for controlling and adjusting the operating voltage of the PV system to be near the MPP under the variable atmospheric conditions. The field of tracking MPP of PV system attracts huge attention from the researchers since it is the best way to increase the harvested energy from the PV system [47]. The drawback of conventional MPPT methods is the incapacity in extracting the maximum power under shading condition. The conventional MPPT methods, such as Perturb and Observe (P&O) [48,49], Hill Climbing and Incremental Conductance (INC) [50,51] (to name a few) is likely to be trapped at one of the local MPPs simply because its algorithm could not differentiate between local and global MPP [52].

Several tracking methods based on optimization approached are proposed for extracting global MPP (GMPP) under PSC. Plenty of reviews on MPPT under uniform and non-uniform solar irradiance are already available. However, most of these reviews simply listed GMPPT techniques based on modern optimization, along with a simple discussion of the advantages and disadvantages of each optimizer without any statistical analysis of cases study. Such shortage is mostly because these reviews aim to cover most conventional MPPT and global MPPT

techniques simultaneously. Accordingly, this review first evaluates the performance of recent works related to twenty global MPPT based on modern optimization approaches. The objectives of this work are as follows:

- Presenting an integrated specific review on the state-of-the-art of twenty global MPPT based modern optimization,
- Comprehensive statistical performance evaluation of various global MPPT algorithms under the same conditions,
- Guide for future work on global MPPT methods via clarifying the pros and cons of each algorithm.

Consequently, the considered global MPPT techniques include: Particle Swarm Optimization (PSO), Differential Evolution (DE), Flower Pollination Algorithm (FPA), Teaching-Learning-Based Optimization (TLBO), Grey Wolf Optimizer (GWO), Water Cycle Algorithm (WCA), Harmony Search Algorithm (HSA), Dragonfly Algorithm (DFA), Mine Blast Algorithm (MBA), Antlion Optimizer (ALO), Imperialist Competitive Algorithm (ICA), Radial Movement Optimization (RMO), Multi-Verse Optimizer (MVO), Whale Optimization Algorithm (WOA), Sine Cosine Algorithm (SCA), Gravitational Search Algorithm (GSA), Cuckoo Search (CS), Firefly Algorithm (FFA), Genetic Algorithm (GA) and Jaya Algorithm (JA). This research is envisaged as a source of valuable information to keep abreast with the modern advance in the field of renewable energy, in addition, to obtain starting on this field for young investigators.

Several types of research done to tackle the global MPPT issue, and their contributions are summarized in Table 1 [53–87].

## 2. Main aspects of partial shading condition

The main issue tackled in this work is studying the impact of PSC on the PVS performance. It is mainly caused by so many factors, such as dust, dirt, clouds, parallel arrays of PV modules self-shading effect, constructions, bird feces, etc [91]. Based on the conducted investigations (Refer to Fig. 1), it can be seen that the shaded cell is subjected to a reverse bias voltage, and it must deliver the same current, usually given by the unshaded one [92]. The resultant reverse power obtained accordingly is accounted for the decrease of the shaded cell output power and consequently, continuous operation under this condition results in the creation of hotspots, leading to an open circuit of the whole PV array [93].

To overcome this problem, frequently, a bypass diode is introduced in parallel with each PV panel to protect the shaded panel, so not being damaged [94,95]. Additionally, another measure is considered with the aim to limit the reverse current, caused by voltage mismatch between the strings; a blocking diode is connected as displayed in Fig. 2-a. The first one increases the complexity of PV characteristics under shading [96,97]. A PV array containing four series connected panels is displayed in Fig. 2-a, while Fig. 2-b illustrates the PV system under shading. As demonstrated in Fig. 2-c, the panel curve includes several MPPs, which may misguide the MPPT to adapt one of this point and operate at it. Obviously, in such a case, the obtained power will be decreased. During normal condition, as illustrated in Fig. 2-c (blue curve), the power-voltage graph has a single peak. Meanwhile, when four solar irradiance levels were considered (Refer to the green curve of Fig. 2-c), the resulting power-voltage graph contains three local points and single global, whilst if the bypass diode is removed, the power-voltage curve will indicate only single peak (red curve). Fig. 2 demonstrates the variation of the PV output power under PSC with and without the bypass diode.

## 3. Global MPPT based modern optimization

In this section, the twenty optimization approaches investigated in this work are reviewed with clarifying the application of each one in

**Table 1**  
Summary of the related works of global MPPT methods.

Author (Year)	Optimizer	Types of Converter	Remarks and main findings
Avila, Pozo (2017) [53]	PSO	Cuk	PV system capacity is 1.2 MW; Integration between PSO and P&O was done; The velocity equation was modified; Very large number of particle swarms are used (300 particles); seven scenarios of partial shading are considered. The integral squared error index is used as a benchmark for comparison between PSO and hybrid PSO-P&O; Using improved PSO decreased the error by 63 % and improved the convergence time (100 msec).
Gavhane, Krishnamurthy (2017) [54]		Boost	Enhanced leader PSO is proposed; Three scenarios of partial shading are considered; Reasonable number of particle swarms are used (5 particles); mutation process is added to conventional PSO and P&O method. A comparison between proposed enhanced PSO and conventional PSO was done; Switching frequency is 10 KHz; the tracking efficiency is enhanced; the tracking speed is increased (10 iterations for PSO and 4 iterations for enhanced PSO).
Liu, Huang (2012) [55]		Buck-Boost	The standard PSO is modified; The PV system capacity is 500 W; the duty cycle of boost converter is used as a particle position; The number of particle swarms is five; The proposed method can reach to global MPP after 27 iteration; The inertia weight is selected as a larger value for better exploration and gradually decrease it for getting good solution; High tracking efficiency greater than 99.5 %
Dwivedi, Mehta [56] (2017) [56]		Boost	PSO is compared with the other traditional MPPT methods. The steady-state fluctuation in power curve is reduced.
Eltamaly et al. (2019) [57]		Boost	The conventional PSO is modified. It became a time-variant global technique. The harvested energy and efficiency of tracking are increased
Farah et al. (2018) [58]		Interleaved Boost Converter	The proposed interleaved boost converter has been compared the conventional boost converter. The deterministic particle swarm optimization is used. Three cases of shading are considered.
Dileep and Singh (2017) [59]		SEPIC converter	Improved PSO is proposed. Experimental work is carried out. The tracking efficiency reached 99%.
Rezk, Fathy (2017) [60]	CS	Boost	The effectiveness of global MPPT under partially shading for two intelligent algorithms PSO and CS have been evaluated. A comparison with INC method has been performed. It has been proved that the performance of CS is better than PSO.
Taheri, Salam (2010) [61]	DE	Boost	The performance of DE under uniform radiation and partial shading has been examined; The proposed algorithm extracted the global MPP with fast-tracking time less than 0.3 s without oscillations; The DE performance compared with classical P&O methods; The simulation results proved that DE has a perfect ability to track MPP accurately with high speed compared with P&O; The population size and the number of generation are 20 and 100 respectively.
Tey, Mekhilef (2018) [62]		SEPIC	Improved DE algorithm is proposed; A modification has been done for ensuring the particles are always compared and converged towards the best particle; the switching frequency is 50 kHz; Load variation condition is considered; Four scenarios of partial shading are considered; The population size is 4; the response time for load variation is one sec.
Kumar, Hussain (2017) [63]		Boost	A combination of DE and whale optimization has been presented; this integration in order to jump out of the stagnation on the local MPP in addition to it decreases the number iterations; The switching frequency is 50 kHz; A comparison with GWO and improved PSO was done; Good capability to track global MPP for all cases was achieved.
Kumar, Hussain (2017) [64]		Boost	The combination between DE and Jaya was proposed; Five scenarios of partial shading are considered; The performance of the proposed hybrid algorithm is enhanced compared with than FPA and PSO.
Ram and Rajasekar (2017) [65]	FPA	Boost	First time introduced FA in the application of global MPPT; Two different configurations of PV system are used; Four scenarios of partial shading are considered; The switching frequency is 10 kHz; A comparison with PSO and P&O was done; The results confirm the FPA superiority compared with others.
Subha and Himavathi (2017) [66]	FPA	Boost	A comparison between FPA and PSO under various shading scenarios is conducted; Ten scenarios of partial shading are considered; The population size is 6; the input voltage of DC converter used as a control parameter; The accuracy and convergence speed have been enhanced through FPA compared with PSO.
Diab and Rezk (2017) [67]			two other optimization methods.
Chao and Wu (2016) [68]	TLBO	Boost	Improved TLBO is proposed; An intelligent teaching factor tuning process for facilitating automatic tunings of TLBO teaching factors is proposed; Four scenarios of partial shading are considered; The population size and the number of generations are 4 and 40 respectively; The tracking performance is improved compared with conventional TLBO and PSO.
Fathy, Ziedan (2017) [69]		Boost	Improved TLBO is presented; During the learner phase, the best learner is nominated as a teacher; A comparison between TLBO and PSO was done. Arduino Uno is used to implementing the algorithm. Improved TLBO succeeded in improving the extracted MPP from the module under PSC; also, it has a high efficiency compared with conventional TLBO and PSO method. The tracking efficiency is 97.5 %.
Patsariya, Rai (2017) [70]		Boost	TLBO is compared with P&O and INC; The PV array contains 50 PV panels; The switching frequency is 5000 Hz; TLBO-MPPT method gave more efficiency as compared to the conventional P&O and IC.
Mohanty, Subudhi (2016) [71]	GWO	Boost	First-time GWO introduced; Two configurations (4S, 2S2P) of PV system are used; Four scenarios of partial shading are considered; Both experimental and simulation works have been conducted; The switching frequency is 25 kHz; A comparison between GWO, P&O and PSO was carried out. The limitations like lower tracking efficiency and steady-state oscillations are removed
Mohanty, Subudhi (2017) [72]		Boost	A combination between P&O and GWO was done; Rapid variation of solar irradiance is considered; Two configurations (3S, 3S2P) of PV system are used; Five scenarios of partial shading are considered; dSPACE 1104 is employed to implement the proposed strategy; A comparison with GWO only and SO+P&O was done; High tracking speed is achieved; faster convergence to global MPP
Sarvi, Soltani (2014) [73]	WCA	Boost	WCA is compared with P&O method in extracting the maximum global power from the partially shaded PV module; voltage is used as a control parameter; The accuracy was improved.
Fathy and Rezk (2016) [74]	MBA	Boost	The performance of mine blast algorithm has been investigated and compared with TLBO under various patterns of partial shading; A comparison with FLC and PSO was done; The duty cycle of boost converter is used as a control parameter; 13 scenarios of partial shading are considered; The tracking speed is enhanced.
Sahu and Shaw (2018) [75]	Antlions	Boost	A comparison between Antlions algorithm and P&O was carried out; Only simulation study; The accuracy and steady state oscillation are improved
Kumar, Hussain (2016) [76]		Boost	Improved Antlions is proposed; Rainy season is considered; ranking technique is added to original Antlions; Five scenarios of partial shading are considered; Experimental and simulation results confirmed that the power extracted is very close to MPP under fast atmospheric fluctuation condition; The average tracking times are 1.18 sec and 1.32 sec respectively for theoretical and experimental investigations.
Vedadi, Vahidi (2015) [77]	ICA	Buck-Boost	Simulation study only considered with three partial shading patterns. A comparison with PSO was done. The convergence speed and accuracy are enhanced.
Seyedmahmoudi an, Horan (2016) [78]	RMO	Cuk	The tracking performance of RMO is compared with PSO; Four factors (convergence speed, efficiency, stability, and computational cost) are considered in the comparison; The switching frequency is 20 kHz; Three scenarios of partial shading are considered; the input voltage of Cuk converter is used as a control parameter; RMO method provided higher speed and efficiency than PSO.
Kumar and Rao (2016) [79]	The whale optimization algorithm	Boost	Three configurations (6S, 3S2P, and 2S3P) of PV system are used; Four scenarios of partial shading are considered; The population size and the number of generation are 6 and 100 respectively; The comparison between WOA, GWO and PSO was done; WOA is superior to GWO and PSO with reference to accuracy and convergence speed.
Kumar et al. (2017) [80]	SCO	Boost	A hybrid approach combined Cauchy and sine-cosine optimization has been presented to simulate the MPPT based on a single current sensor; A battery charging system is used as a load; The cost of the charging system is decreased; A comparison with GWO was done; The switching frequency is 50 kHz; Three scenarios of partial shading are considered; The tracking performance is enhanced
Saha (2015) [81]	GSA	Boost	Gravitational search algorithm is employed to design MPPT with PV array in comparison with PSO; The voltage is used as a control parameter; The population size and the number of generations are 10 and 50 respectively; the tracking time is 0.006 sec; the tracking performance is improved compared with PSO
Zheng et al. (2011) [82]	Tabu search algorithm	Boost	Tabu search with three presented search stage, diversification, local and intensification has been presented to simulate the MPPT of PV system operated under partially shaded conditions; Initial population size and radius of the Tabu ball are 4 and 5 respectively; Three scenarios of partial shading are considered
Sridhar et al. (2017) [83]	SFLA	Boost	First time SFLA is used for global MPPT incorporated with partially shaded PV system; The approach is compared with P&O and PSO; the SFLA-MPPT enhances the GMPP about 30% than that obtained via P&O; The PV voltage is used to drive PID to generate the duty cycle of the DC converter; The main drawback of the proposed system, it needs four sensors (current, voltage, temperature, and radiation) to reach global MPPT; Three scenarios of partial shading are considered

(continued on next page)

Table 1 (continued)

J. Ahmed, Z. Salam et al. (2014) [84]	CS	Buck-Boost	The CS has been performed for MPPT with partial shading capability (PSC) in PV scheme in different scales. The performance of CS has been compared to PSO and P&O techniques. Although CS calculation is very complex as compared with PSO technique, the simulation results illustrate that the CS executes perfectly than the other two that is very fast with a steady state attitude using fewer tuning parameters.
Sundareswaran et al. (2014) [85]	Flashing firefly algorithm	Boost	FA is proposed for MPPT via PSC. According to the simulation results, the FA has perfect tracking attitude as compared to PSO and P&O techniques. Notwithstanding, standard FA contains several inherent issues.
Teshome et al. (2017) [86]		Boost	A modified FA is implemented for MPPT under PSC. The MFA is compared to the FA, PSO, and P&O techniques. MFA technique is very effective to track the global MPP. The median improvement of MFA in tracking accuracy/speed can be almost 1.7 times the FA. Moreover, MFA has perfect tracking attitude than the other two techniques.
Hadji et al. (2011) [87]	GA	Boost	GA optimized the parameters of the fuzzy-logic controller depending on MPPT for PV scheme. It has been performed comprehensive analysis with P&O, and Incremental Conductance (INC) techniques; GA optimized MPPT scheme introduced perfect tracking precision as compared to others.
Ramaprabha et al. (2011) [88]		Boost	The MPPT controller has been controlled based on artificial neural network (ANN) optimized via GA; GA extracted MPP from Solar photovoltaic (SPV) source. The optimized values of power and voltage for different insolation levels and temperatures have been used for training the ANN. The offline training of ANN by GA has been used to produce the reference voltage corresponding to the MPP for any environmental change.
Bakhshi et al. (2014) [89]		DC/AC inverter	The proposed GA has been employed for constructing a power plant station with various inverters. In this regard, a novel methodology depending upon GA has been implemented evaluating the optimum inverter capacity in addition to, the configuration of the scheme for grid-connected photovoltaic models via array capacity that is established in advance.
Huang et al. (2018) [90]	S-Jaya Algorithm	Boost	The S-Jaya technique has been proposed for overcoming effectively the MPPT issue of PV schemes via PSC. It has been considered that the PV scheme manages the produced power via its output voltage. S-JA has been compared with standard JA and PSO. The results have been illustrated that the S-JA has higher convergence speed and tracking efficiency.

extracting the GMPP for the partially shaded PV array. Additionally, the limitations of each approach are included.

3.1. Particle Swarm Optimization (PSO)

PSO was firstly proposed by Kennedy and Eberhart [98,99]. This technique is considered as the most powerful tool compared with the various MPPT algorithms, this is due to its high computational speed, simple concept, easy application, excellent accuracy and possibility to be applied for nonlinear problem optimization. Therefore, sufficient solution of multiple MPPs under partial shading can be obtained compared with other methods [100]. The basic concept of PSO is motivated from the crowded bird's behavior or schooling fishes [101]. PSO implies some particles forming a swarm wandering wasps around the search space to identify the optimal solution. Due to their acquired flying experiences, each particle tries to adjust its traveling velocity. The theoretical concept of PSO is based on identifying definite zone named solution space and each of them accumulates a potential problem solving degree. At stage one, several randomly distributed particles in the search area are assumed to be saved in the initial best position. The idle positions of all will be saved as the global perfect ones. After that, a step size is modified for these particles. Next, the cost function is estimated for every particle and compared with previous values. Finally, the previous steps are repeated until reaching matching outcomes [102]. Fig. 4 explains the updating process of the particle position [103]. Fig. 5 shows the searching procedures and flowchart of PSO [104].

PSO is applied on extracting GMPP from PV array via considering the converter duty cycle while the output power is considered as the objective function. The converter duty cycle ( $d_i$ ) is regulated and updated using the following eqns and Fig. (3) [104,105]:

$$d_i^{k+1} = d_i^k + \Phi_i^{k+1} \tag{1}$$

$$\Phi_i^{k+1} = w\Phi_i^k + k_1 r_1 \{P_{best} - d_i^k\} + k_2 r_2 \{G_{best} - d_i^k\} \tag{2}$$

where  $\Phi_i^{k+1}$  is the step size,  $k_1$  and  $k_2$  are the acceleration coefficients,  $w$  is the inertia weight,  $r_1$  and  $r_2$  are random values in range [0, 1].

At the beginning, a population represents the duty cycle is initialized and the corresponding voltage and current are measured and then the power is calculated, the duty cycle is then updated based on eqns. (1) and (2) and the corresponding power is extracted [106]. The updating process is performed in case of increasing power; the process is repeated until the maximum global power is obtained.

3.2. Differential Evolution (DE)

This algorithm is suggested by Storn and Price in 1995 in their efforts to introduce a superior optimization tool [87]. The algorithm is categorized into three steps, specifically: mutation, crossover, and selection. In MPPT implementations, the PV power represents the fitness function. Meanwhile, the converter duty cycle is used as a target vector  $d_i$ . Initially, the population is arbitrarily generated. Any single particle inside population can be assumed to be a possible solution [87]. On the process, the initially generated duty cycles are used with PV, and then consequently, the PV power,  $P_i$ , is determined depending on the measured PV current and voltage. Next, the highest power is nominated as  $P_{best}$  and its corresponding duty cycle is selected as the best value ( $d_{best}$ ) [107]. During the mutation phase, the donor vector,  $d_{vi}$ , is created using the following eqn:

$$d_{vi} = D_{best} + F * (d_{r1} - d_{r2}) \tag{3}$$

where  $r_1$  and  $r_2$  denote random integers,  $F$  denotes scaling operator.  $d_{r1}$

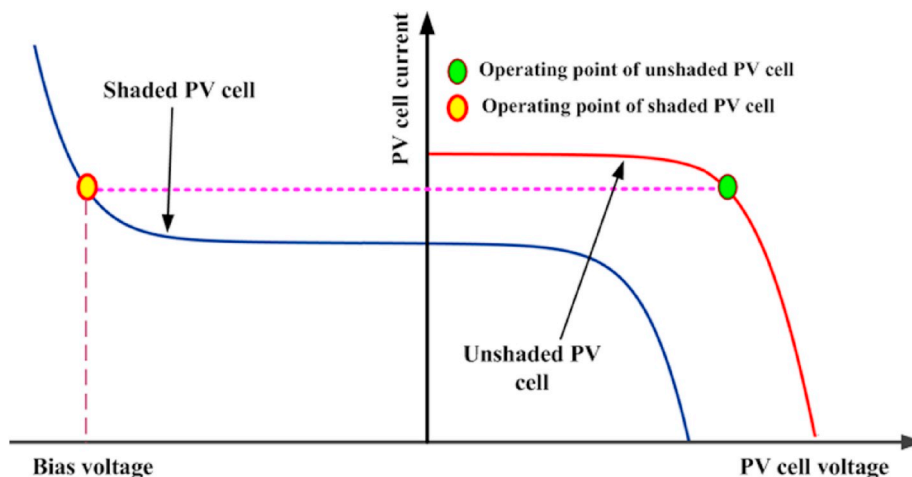


Fig. 1. The current, voltage characteristics of PV solar cell.

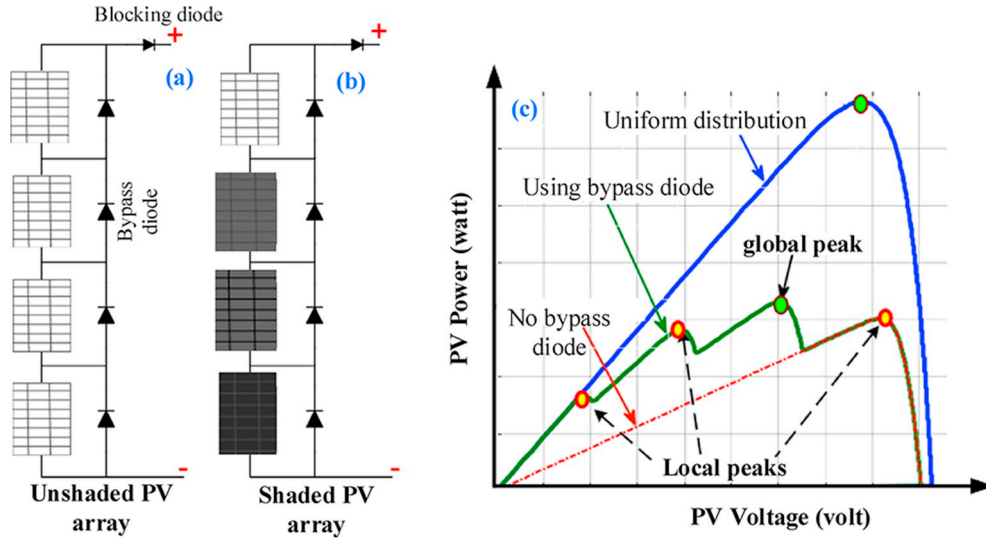


Fig. 2. (a) Unshaded PV array (b) Shaded PV array (c) power against voltage graphs.

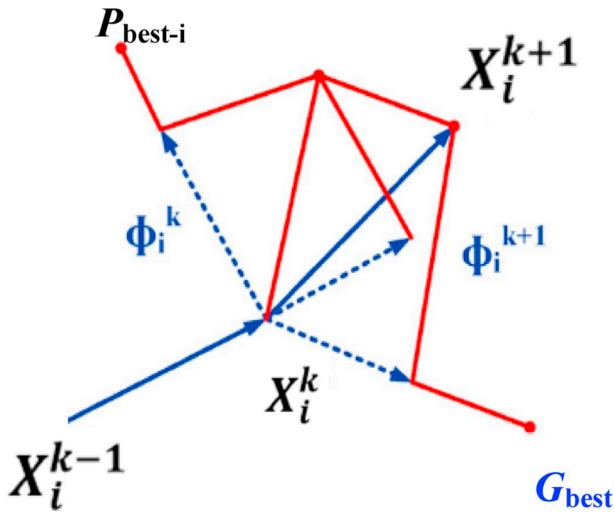


Fig. 3. Update process for the position of particle.

and  $d_{r2}$  represent the selected vectors by random way.

Then the resultant vector is limited according to the maximum and minimum boundaries as follows:

$$dv_i = \begin{cases} dv_i = d_{max} & \rightarrow \text{if } dv_i \text{ greater than } d_{max} \\ dv_i = d_{min} & \rightarrow \text{if } dv_i \text{ smaller than } d_{min} \end{cases} \quad (4)$$

Next, the crossover phase is started. During this phase, the trail vector is created based on the following eqn:

$$du_i = \begin{cases} dv_i & \text{if } rand \leq C_r \\ d_i & \text{otherwise} \end{cases} \quad (5)$$

where  $C_r$  is the control parameter of crossover.

Final phase is the selection phase. The cost functions corresponding to trial and target vectors are compared. Based on the best cost function, the best vector is selected to continue in the next iteration based on the following relation [108]. The duty cycle of higher amount of power is utilized as the next target vector as follows:

$$d_{i+1} = \begin{cases} du_i & \text{if } f(du_i) \geq f(d_i) \\ d_i & \text{otherwise.} \end{cases} \quad (6)$$

The searching procedures of the algorithm are illustrated in Fig. 5.

### 3.3. Flower Pollination Algorithm (FPA)

FPA is introduced in 2012 by Xin Yang [109]. This approach is motivated from the action of flower pollination. The term of pollination can be defined as the physiological process of plants mating. In general, there are two kinds of pollination namely self and cross pollination. Self-pollination is happened when pollen of one flower fructifies the same flower or another flower in the same kind of plant. Whereas, cross-pollination occurs when grains of pollen moved from various plant [65]. The two common methods to prevalence the pollen between flowers are abiotic and biotic pollination. The abiotic pollination is occurred by the help of wind and rain. Moreover, this kind account 10% off pollination and it is notrequired for any pollinators. The biotic pollination occurs by the help of birds and animals and accounts 90% of pollination [65]. Four rules must be taken under consideration for designing and implementing the FPA algorithm. Firstly, Biotic- and cross-pollination are considered as global pollination process and may occur over a large distance where levy flights are utilized for transfer pollens. Secondly, abiotic- and self-pollination are considered as local pollination. Thirdly, flower constancy is deemed as production possibility proportional to the matching among two flowers involved. Finally, the occurrence of both local and global pollination have controlled and monitored using switch probability [65,66]. According to the previous four steps, the mathematical model can be represented as follows:

The characteristic equation of global pollination and flower constancy from the first rule and third rule is given as follow:

$$x_i^{t+1} = x_i^t + \gamma L(\lambda)(g_* - x_i^t) \quad (7)$$

where  $x_i^{t+1}$  is the pollen for the same kind of flower at iteration  $t$ ,  $g$  is the best value of duty cycle,  $\gamma$  is scaling factor that utilized for making controlon step size and  $L(\lambda)$  is Lévy flights which is accountable to move apollens to various kinds of flowers and assist to enhance the pollination strength and determined by the following:

$$L \approx \frac{\lambda \Gamma(\lambda) \sin\left(\frac{\pi\lambda}{2}\right)}{\pi} \frac{1}{s^{1+\lambda}} \quad (s \gg s_0 > 0) \quad (8)$$

Here  $\Gamma(\lambda)$  represents the gamma function.

The characteristic equation of local pollination from the second and third rule is given as follows [65]:

$$x_i^{t+1} = x_i^t + \epsilon(x_j^t - x_k^t) \quad (9)$$

where  $x_j^t$ ,  $x_k^t$  are pollen from various flowers of the same kind of plant and  $\epsilon$  is epsilon and its value between 0 and 1.

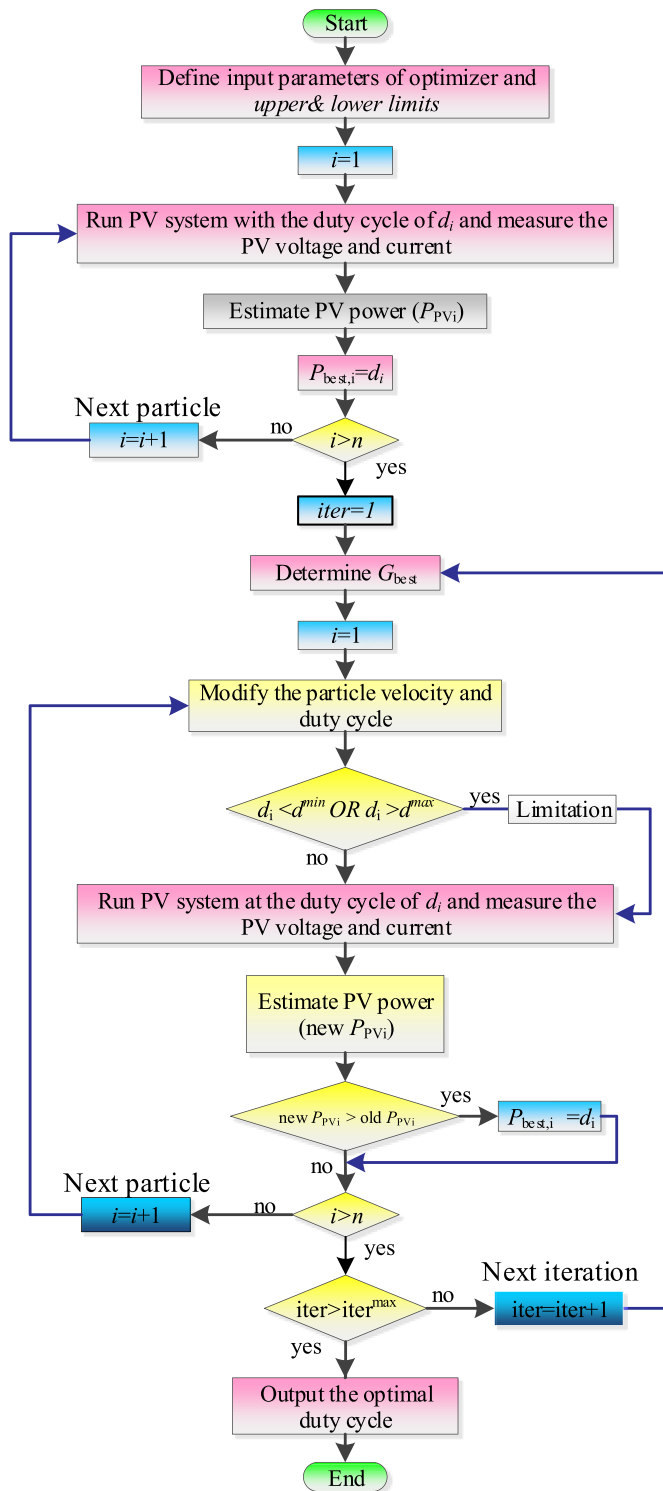


Fig. 4. Flowchart for mechanism searching using PSO method.

Fig. 6 shows the schematic chart of flower pollination method [67]. Firstly, the approach initializes its controlling parameters with upper and lower bounds of duty cycle with tracking the value of PV output power. The maximum power is selected as the best one, and then the donor vector of duty cycle is generated, the later is fed to the converter with measuring the corresponding power, the updating process is taken place in case of power increase.

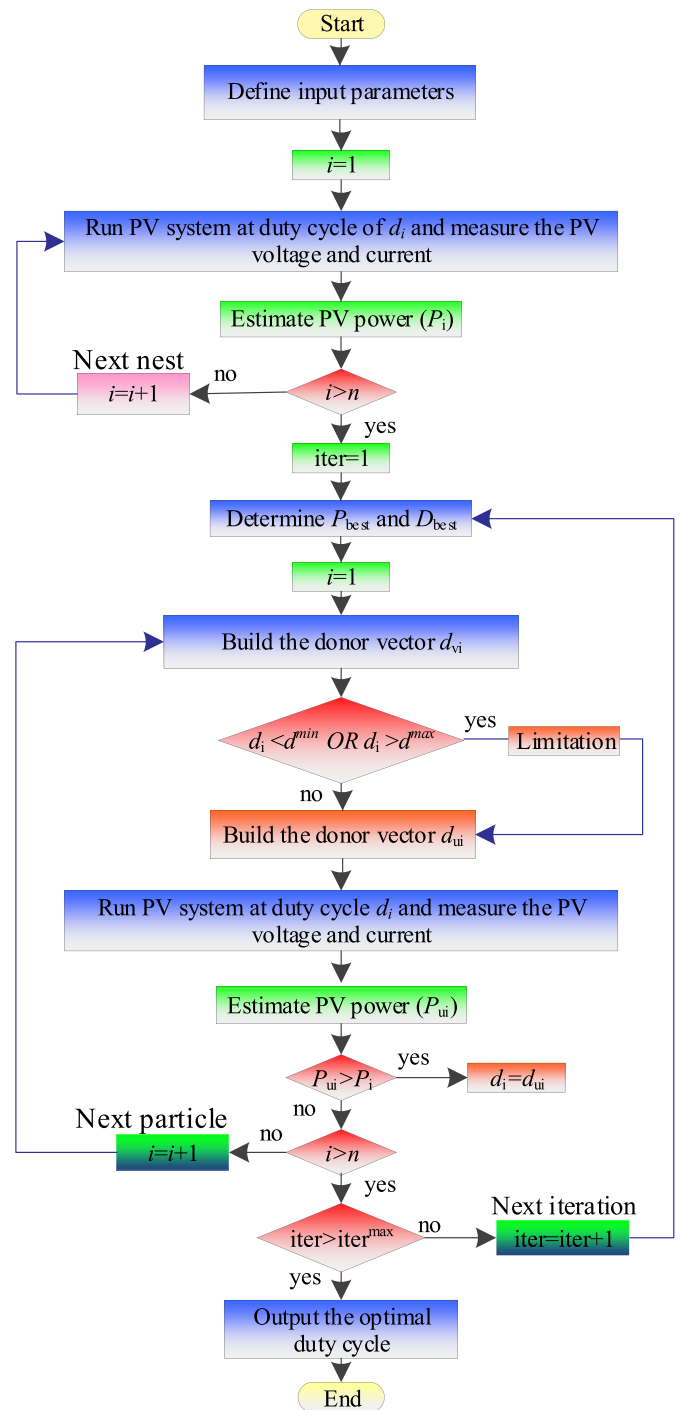


Fig. 5. The searching procedure of DE algorithm.

### 3.4. Teaching-learning-based optimization (TLBO)

TLBO was suggested in 2011 by Rao et al. [68,110]. The basic idea of this method is to emulate the learning process among the teacher and his learner (student). Several learners represent the population and various subjects educated to them. The different subjects represent the various design of variable where the fitness function is represented as the outcome of learners. TLBO process comprises the learner phase and teacher phase. Through these two phases, the teacher tries to raise the learner's level by improving the knowledge. In the teacher phase, the teacher tries to fetch the learner's level toward or more his knowledge level which is done by increasing the mean rate of learners,  $M_i$ , to his

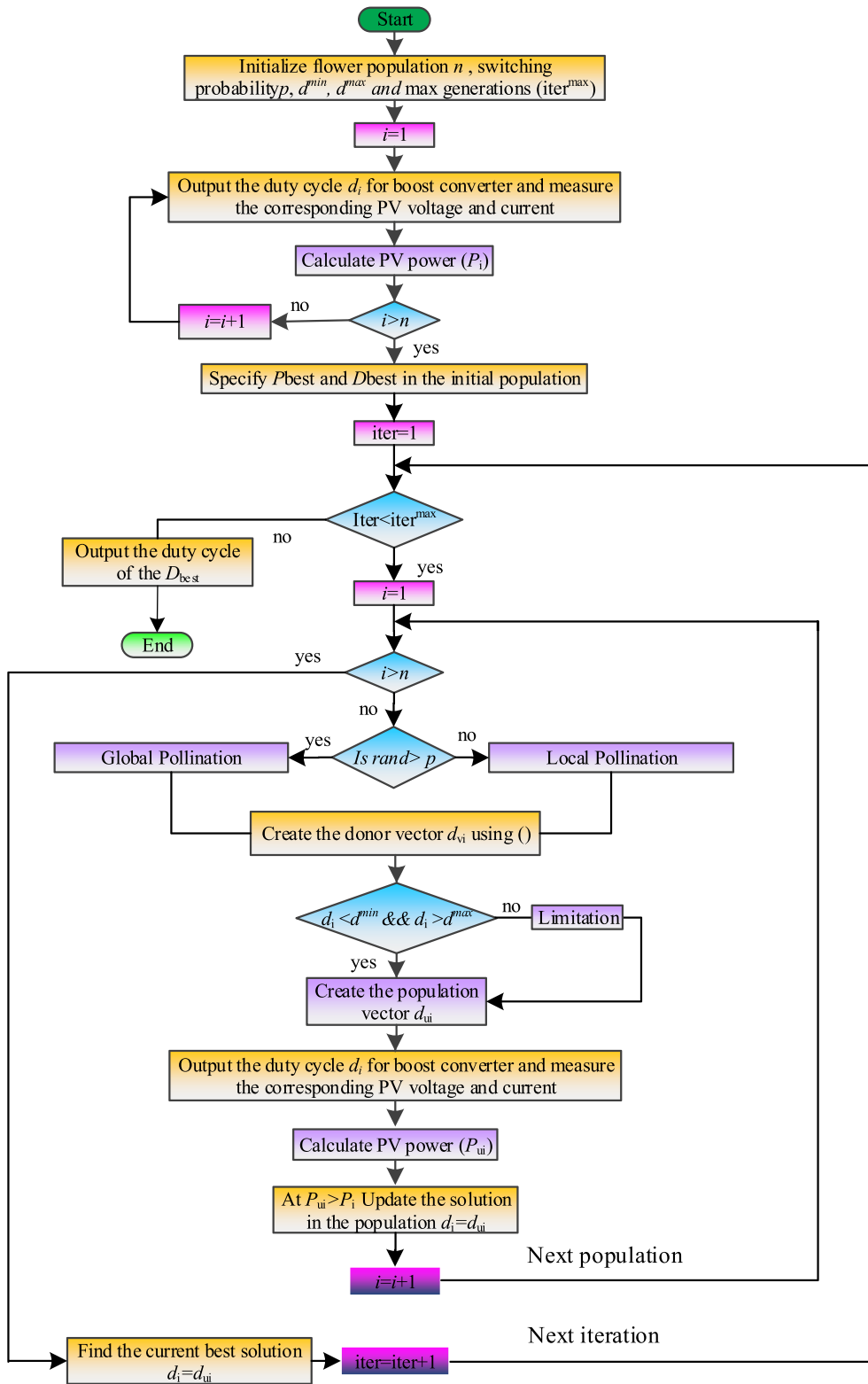


Fig. 6. Flowchart of flower pollination method.

level rate of means  $M_{new}$ . The learners' rate is enhanced based on the difference between the present and desirable mean as follows [111,112]:

$$diff_{mean\ i} = r_i * (M_{new} + T_f * M_i) \tag{10}$$

where  $r_i$  is the random number between [0,1],  $T_f$  represents the teacher factor that may equal 1 or 2 and calculated as follows:

$$T_f = round(1 + rand(0,1)\{2 - 1\}) \tag{11}$$

The updated value of present learners,  $X_{new,i}$ , depends on the amount of different means between the present and desirable solution, it can be determined as follows:

$$X_{new,i} = X_{old,i} + diff_{mean\ i} \tag{12}$$

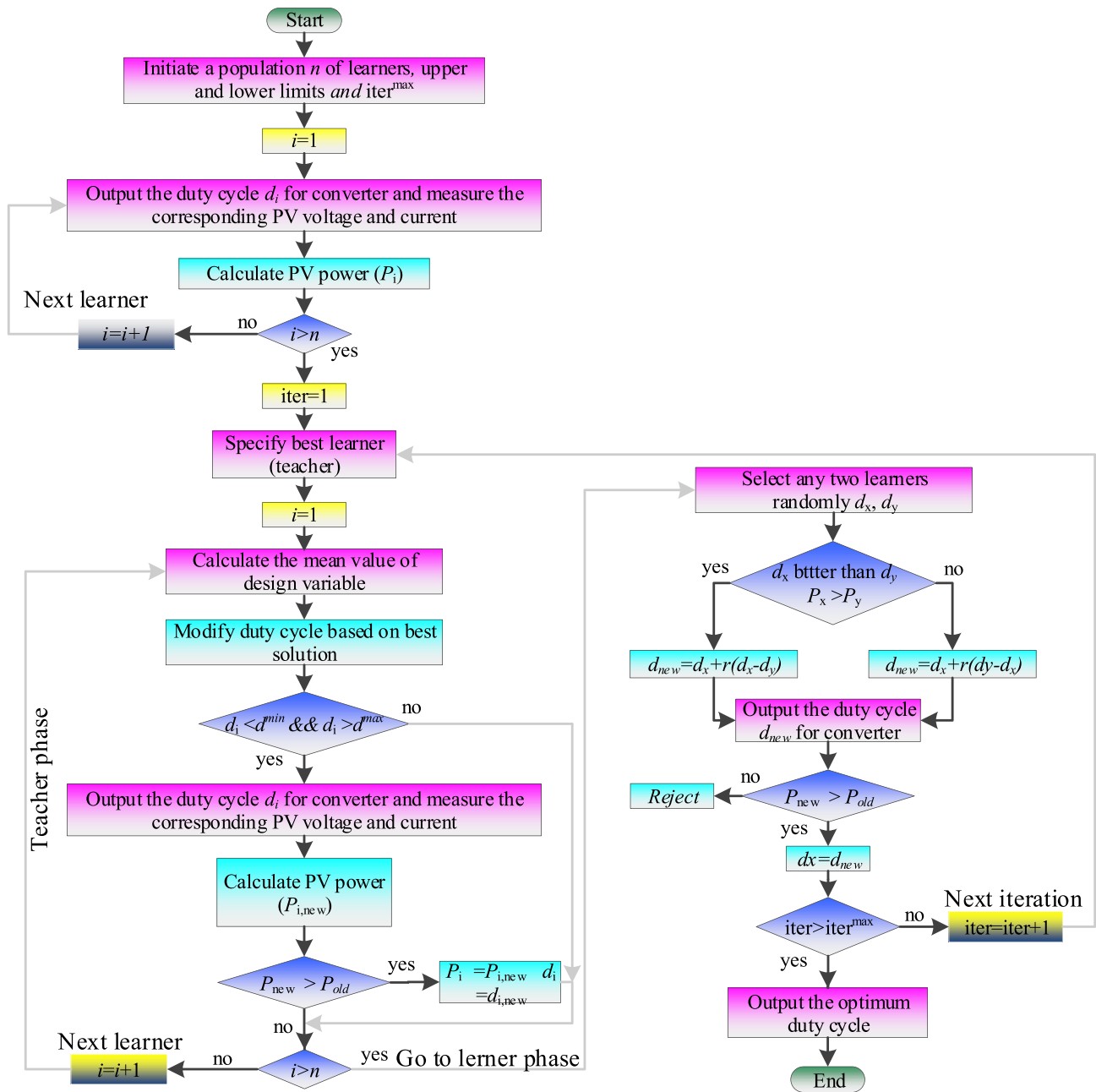


Fig. 7. Flowchart of Teaching-learning-based optimization method.

In the learner's phase, improving the knowledge for a student is done by two ways, the first way occurs through interaction between the learners inside the class. Whereas the input knowledge in the second way is taken from the teacher. The updating process is considered when the other learner in class has more knowledge than the rest of students and the modification of learners is expressed randomly by choosing two learners and comparing between them as the follows [111]:

$$\text{IF } f(X_i) > f(X_j) \text{ then } X_{new,i} = X_{old,i} + r_i(X_i - X_j) \quad (13)$$

$$\text{else } X_{new,i} = X_{old,i} + r_i(X_j - X_i) \quad (14)$$

The value of  $X_{new,i}$  is accepted if it achieves better performance than the old one.

Fig. 7 explains the process of teaching-learning-based optimization approach [68].

### 3.5. Grey wolf optimization (GWO)

GWO is introduced by Mirjalilis [113]. It mimics the social hierarchy and mechanism of hunting the grey wolves [114]. In general, the hunting of grey wolf has done according to three steps, searching for prey then encircling prey and finally attacking prey. Grey wolves are subdivided to four levels, the first one is leader which also named alphas ( $\alpha$ ) wolves and these wolves give the best solution for the optimization problems. The second and third better solution are called beta ( $\beta$ ) and delta ( $\delta$ ) wolves respectively. The final level is called omegas ( $\omega$ ) wolves which are deemed as the lowest degree in grey wolves. In the fact, the cooperation and good communication among wolves help in obtaining the optimal solution in less interval of time [114–116]. The GWO provides several advantages like high tracking efficiency, no steady state oscillations, the parameter that required for adjustment are fewer and robust. On the other hand, the high cost, complexity and, big search space are considered as the major drawbacks of this technique

[72,117]. The alphas ( $\alpha$ ) wolves are considered as the fittest solutions. Beta ( $\beta$ ) and delta ( $\delta$ ) wolves are considered as the best solution receptivity after ( $\alpha$ ). However, omegas ( $\omega$ ) are assumed to be the residue of the candidate solution. During the period of hunt, the grey wolves surround the prey and the behavior of encircling can be modeled mathematically as follows [118]:

$$\vec{D} = |\vec{C} \cdot \vec{X}_p(t) - \vec{X}(t)| \quad (15)$$

$$\vec{X}(t + 1) = \vec{X}_p(t) - \vec{A} \cdot (\vec{D}) \quad (16)$$

where  $t$  is the current position,  $\vec{X}_p$  is the position vector of prey,  $\vec{X}$  is the position vector of grey wolves,  $\vec{A}$  and  $\vec{C}$  indicate the coefficient vectors and calculated as follows [71]:

$$\vec{A} = 2\vec{a} \cdot \vec{r}_1 - \vec{a} \quad (17)$$

$$\vec{C} = 2 \cdot \vec{r}_2 \quad (18)$$

where  $\vec{r}_1$  and  $\vec{r}_2$  are random vectors in period [0, 1],  $\vec{a}$  is the component vector that decreased from 2 to 0 through the course of iterations.

In GWO, the hunting process is done by  $\alpha$ ,  $\beta$ , and  $\delta$ . Whereas, the track of three wolves is presented by  $\omega$  wolves. The three wolves  $\alpha$ ,  $\beta$ , and  $\delta$  are considered as wolves that have better knowledge about the potential of prey position. Furthermore, the other search agents update their locations agreeing to the position of the best search agent as explained as follows [114,119]:

$$\vec{D}_\alpha = |\vec{C} \cdot \vec{X}_\alpha - \vec{X}|$$

$$\vec{D}_\beta = |\vec{C} \cdot \vec{X}_\beta - \vec{X}|$$

$$\vec{D}_\delta = |\vec{C} \cdot \vec{X}_\delta - \vec{X}|$$

$$\vec{X}_1 = \vec{X}_\alpha - \vec{A}_1 \cdot (\vec{D}_\alpha)$$

$$\vec{X}_2 = \vec{X}_\beta - \vec{A}_2 \cdot (\vec{D}_\beta)$$

$$\vec{X}_3 = \vec{X}_\delta - \vec{A}_3 \cdot (\vec{D}_\delta)$$

$$\vec{X}(t + 1) = \frac{\vec{X}_1 + \vec{X}_2 + \vec{X}_3}{3} \quad (19)$$

The following steps describe the main principle operation of GWO approach.

- (1) The initial population is generated randomly,
- (2) The possible position of prey through iterations is calculated by  $\alpha$ ,  $\beta$ , and  $\delta$  wolves,
- (3)  $\vec{a}$  is linearly decreased from 2 into 0 to search about prey and also for attacking the prey respectively. When  $|\vec{A}| > 1$ , the candidate position moves far from the prey and moves toward the prey when  $|\vec{A}| < 1$ ,
- (4) Searching process is stopped when the end criterion is met.

Figs. 8 and 9 show the position updating of the grey wolf and its flowchart.

In GWO approach, it is combined with direct duty-cycle control, i.e., on the MPP, duty cycle is sustained at a constant value, in each iteration the converter duty cycle is updated based on eqn. (19) until converging with the global MPP.

### 3.6. Water cycle algorithm (WCA)

WCA or hydrological cycle was introduced by Eskandar [120]. The principle of WCA explains the continuous of water moving below or above the earth surface. It comprises from diverse phase like evaporation, runoff water on surface and precipitation. In general, the stream

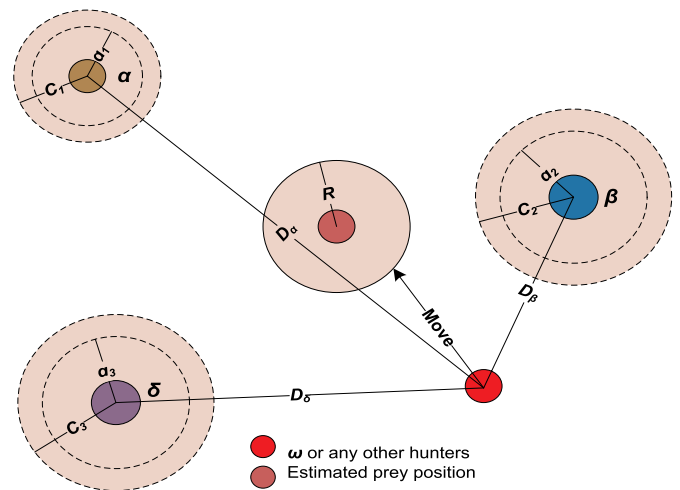


Fig. 8. Position updating for grey wolf optimization method [114].

influxes into rivers and the rivers influxes into the sea. One of the major features of WCA is requirement of lower tuning number parameters. Therefore, it has good ability to resolve massive optimization issues with constant parameters [120,121]. The initial population or stream population is randomly generated after the process of raining. The sea is chosen as the best individual and river is considered as the number of good individual, while the rest represents the stream. The streams are generated from raindrops which form river after joint with other. In addition, some streams flux directly to the sea (best solution). Fig. 10 shows the diagram of the streams flux towards specific river along connection line of distance  $d$ . Furthermore, the same concept can be utilized in fluxing river to the sea.

Both streams and rivers positions can be updated based on the following eqns [120,121]:

$$x_{Stream}^{t+1} = x_{Stream}^t + rand \times C \times (x_{River}^t - x_{Stream}^t) \quad (20)$$

$$x_{River}^{t+1} = x_{River}^t + rand \times C \times (x_{Sea}^t - x_{River}^t) \quad (21)$$

where  $x_{Stream}^t$ ,  $x_{River}^t$  and  $x_{Sea}^t$  are the positions of streams, rivers, and sea at iteration number  $t$ ,  $rand$  is a random number in range [0, 1] and  $C$  is chosen as 2 in the analysis. In WCA, voltage at maximum power is compared with the actual PV terminal voltage, the system incorporates PID controller represents MPPT which is responsible for calculating the reference voltage at maximum power.

### 3.7. Harmony search algorithm (HSA)

This optimization algorithm, which is based on a band musical performance [122], was suggested primarily via Geem in 2001 discovering the most suitable harmony-case in terms of the beauty's nature. It gained magnificent attention because of its balance amalgamation between exploration and exploitation, in addition from carrying out viewpoint [123]. The HSA technique is executed for various optimization issues like vehicles routing, design of truss structure and calibration of hydrological parameters. Generally, there is no need of primary amount of the harmony algorithm for resolution variables, utilizing random quest based on the prospect of harmony mind and the degree of pitch-modification. As well, such meta-heuristic imposes minimal arithmetical necessities that make it suitable for dissimilar patterns of optimization issues. The major stages of HSA are illustrated in Fig. 11.

### 3.8. Dragonfly Algorithm (DFA)

DFA is based on replicating the flight motion of dragonflies' swarm. Dragonflies are considered as fancy insects. Generally, they are

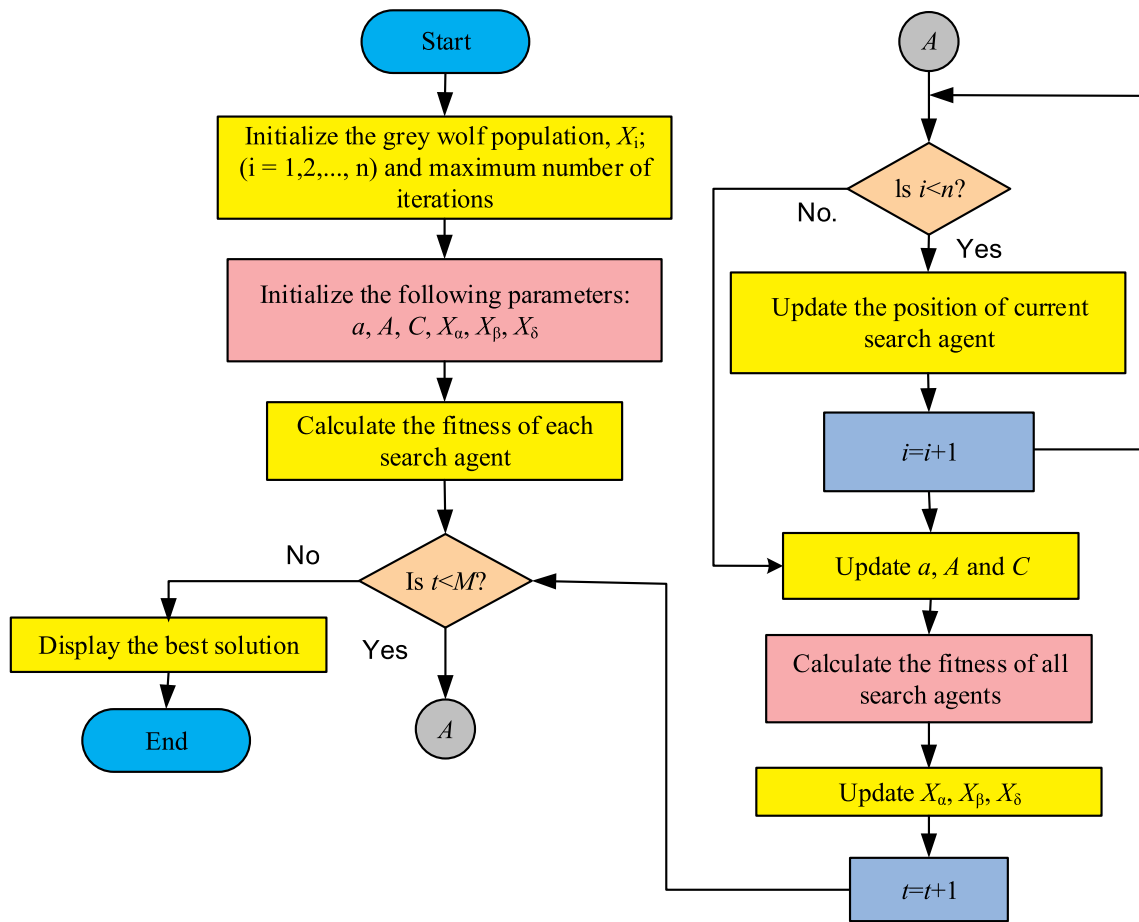


Fig. 9. Flowchart of Grey Wolf Optimization method.

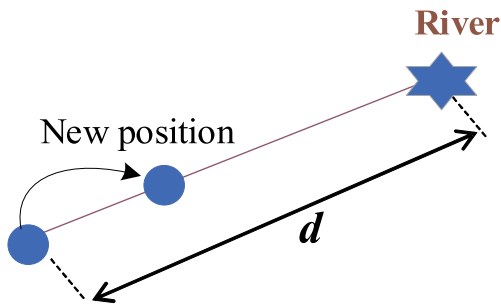


Fig. 10. Stream's movement toward the river.

approximately 3000 different species around the world of this insect. The life cycle of dragonflies includes two major milestones namely, nymph and adult. The main part spends of life span done in nymph then transfer to be adult [124,125].

Dragonflies almost hunt all small insects found in nature. Therefore, these kinds are considered as small predators. They are two purposes for dragonflies' swarm; hunting, which is also called static swarm and migration, which called dynamic swarm. Dragonflies make little groups and fly over small and various regions to catch preys like butterflies in the mode of static swarm. The major characteristics of the static swarm are the local movement and sudden change in direction path through flying. However, the dragonflies create a swarm for migrating in one position over along space distance in dynamic phase [126,127]. The model of search agent motion is executed after integrating five main individual style in swarm named; separation ( $S_i$ ), alignment ( $A_i$ ), cohesion ( $C_i$ ), attraction to food source ( $F_i$ ) and distraction faraway from preys ( $E_i$ ) [127]. The swarm comprises from  $N$  dragonflies that deem as

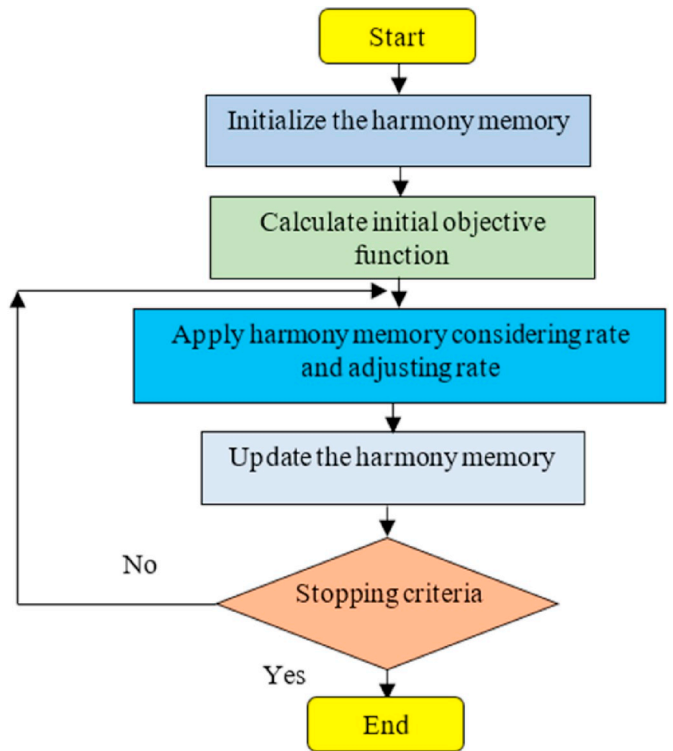


Fig. 11. Flowchart of Harmony search algorithm.

search agents. For updating the dragonflies in the search area and for simulating the motion of dragonflies, two main vectors are considered namely  $\Delta X$  (step vector) and  $X$  (position vector). The step vector utilized in DFA is similar to velocity vector in PSO method and this vector provides a good location of motion of dragonflies. The calculation of step and location for every search agent can be represented by the following [124]:

$$\Delta X_i(k+1) = sS_i(k) + aA_i(k) + cC_i(k) + fF_i(k) + eE_i(k) + \omega\Delta X_i(k) \quad (22)$$

$$X_i(k+1) = X_i(k) + \Delta X_i(k+1) \quad (23)$$

The behaviors fitness values of search agent  $i$  are  $S_i$ ,  $A_i$ ,  $C_i$ ,  $F_i$ , and  $E_i$ , and the weights of the behaviors are  $\omega$ ,  $a$ ,  $c$ ,  $f$ , and  $e$ . Within the context of GMPP of PV systems, the location of the dragonfly is the duty cycle at which the converter operates and the goal feature to be optimized is the power output of the PV array.

### 3.9. Mine blast algorithm (MBA)

MBA was presented by *Sadollah*, the approach is motivated from the observation of the phenomenon of mine bombs that produce a very small segment of shrapnel. The probable ideal solution is deemed as the large explosive mine. The exploration and exploitation are the two main processes of MBA. Pseudo code of this algorithm is shown in Fig. 12. Finding the most mine explosive, which is situated at the ideal position, is the major function of this algorithm. The algorithm starts by finding the initial point which is also named shot point,  $X_0^K$  ( $K$  represents the number of shot points), that generated a number of shrapnel segment  $N_s$  [74]. The ideal solution of this method is done by minimizing the distance between shrapnel pieces. This achieved through  $\alpha$  (reduction constant) which is defined by the user. The reduction of initial distance can be calculated based on the following eqn [74].:

$$V_j^k = \frac{V_j - 1}{\exp\left(\frac{k}{\alpha}\right)} \quad (24)$$

where  $V_j^k$  indicates the distance of the produced shrapnel pieces for each iteration  $k$ . In MPPT based MBA, the shrapnel pieces are the converter duty cycle fed to converter while the fitness function is the PV array output power, the updating process for duty cycle is performed with reducing the distance based on eqn. (24) until the global power is obtained.

```

Initialize the population and first shoot point,
While (i< max_iteration)
Calculate the exploding mine blast's location,
If exploration factor < max_iteration
Compare with global solution
Else
Return to step 3
If initial shrapnel pieces' distances are reduced,
K=k+1
Else
Stop
End
Print optimum solution

```

Fig. 12. Pseudo code of mine blast algorithm.

### 3.10. Antlion optimizer (ALO)

*Mirjalili* suggested ALO; this algorithm mimics the mechanism of hunting for antlion in nature. The antlions make a hole in the sand that has cone-shaped over a circular path. After that, the antlion stows in the bottom of the cone and waits the prey to trap inside the hole and tries to catch it. In general, the insects did not immediately caught and attempted to get away from the trap. However, the antlions intelligently throw the sands to the edge of the hole to force the prey to slip into bottom. And, finally, based on the old trap information, the antlions try to build a good new hole [128,129]. The size and diameter of the hole rely on the rates of hunger and the size of moon. The updating position of ants can be represented as follows [128]:

$$Ant_i^k = \frac{R_A^K + R_E^K}{2} \quad (25)$$

where  $R_A^K$  denotes the random walk beside the antlions,  $R_E^K$  denotes the random walks around elite at iteration  $K$ .

Fig. 13 shows the schematic diagram of antlions for hunting behavior process and its pseudo code [76].

ALO has been applied to extract the global MPP of the PV module underneath partially shaded situations in comparison with P&O algorithm. It is shown that, the manipulate model of the PV module primarily based on ALO supplied worldwide MPP tracking with real-time manipulate speed and a steady very last value of the output electricity of a partially shaded PV module.

### 3.11. Imperialist competitive algorithm (ICA)

ICA is considered as recent and attractive metaheuristic optimization approach for solving complicated nonlinear optimization problems, it was presented by *Gargari* and motivated from the idea of the imperialistic competition process. This approach starts with randomly generating initial population or empire. Every individual in the empire is named a country and the countries are classified into two kinds; imperialist states which have the best value of fitness function and colonies which are pursuing the imperialists [77]. Some of best countries between populations are chosen to be imperialist and the reminder of other population is comprised between the mentioned imperialist as colonies. The lowest empire that cannot maximize its power and also cannot succeed in the competition will be excluded from the competition. As a result, all colonies try to move toward their pertinent imperialists according to the competition between empires. Finally, the breakdown mechanism will hopefully cause all the countries to become close to a state in which just one empire is existed in the world, and all the other countries become colonies of the empire. The solution will be obtained by the robust empire [130]. Fig. 14 Explains the motion of colonies in random action to the relevant source of imperialist [130].

Fig. 15 presents the pseudo code for imperialist competitive algorithm.

The motion of colonies towards the location of imperialist relies on the distance ( $d$ ) between them. The new colony position is calculated by eqn. (26), this process depends on the distance between the colonies and their imperialists. The new position of the colony is calculated by Ref. [131]:

$$x^{k+1} = x^k + \gamma \cdot \delta \cdot d \quad (26)$$

where  $x^{k+1}$  is the new position of colony at iteration  $k+1$ ;  $x^k$  is the position of colony at iteration  $k$ ;  $\gamma$  is the assimilation coefficient,  $\delta$  is the random value in range [0, 1] and  $d$  is a vector that denotes the distance between colony and its imperialist. ICA has been applied to track the GMPP of PV string under partially shaded condition using different sets of shadow patterns. The DC-DC converter duty cycle is set for maximizing the PV array output power.

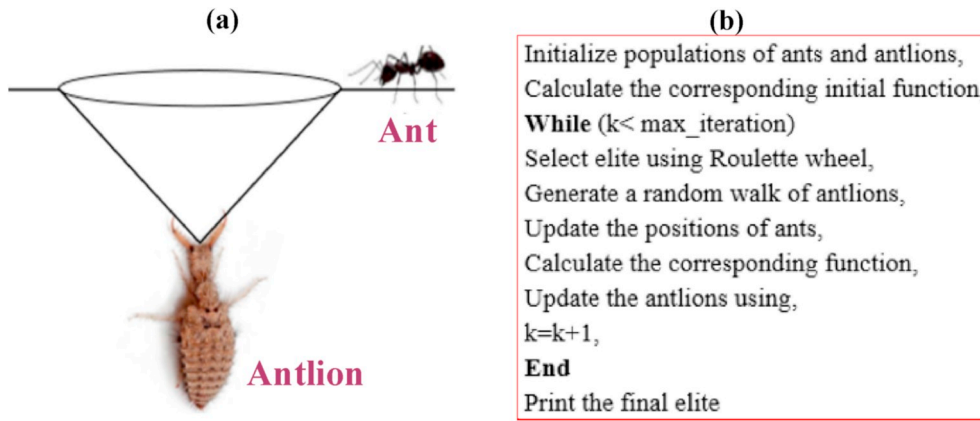


Fig. 13. (a) Schematic diagram for antlions for hunting behavior; (b) Pseudo code of antlions algorithm.

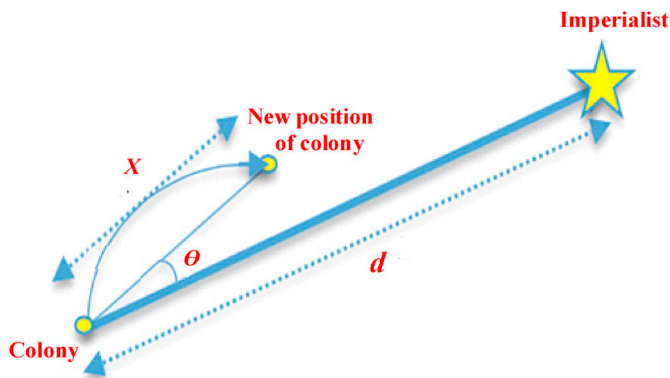


Fig. 14. Movement of colonies to the relevant source of imperialist in ICA (A) regular motion toward new location (B) in random action toward new location.

### 3.12. Radial movement optimization (RMO)

RMO can be considered as swarm based stochastic optimizer that has numerous resemblances to the most famous evolutionary algorithms like PSO and DE. Such a technique is performed in 2014 by Rahmani et al. [132,133]. The main difference between evolutionary algorithms and RMO is that the particles are transferred closely to a middle position that is brought up to date at every iteration [52]. This technique produces many merits like its speed-convergence is very high and it has very high effectiveness. Also, the degree of complexity and the construction investment are minimal and the balance of attitude in following up as comparing other metaheuristic algorithms [132]. One of the advantages that differentiate such technique over another metaheuristic methods is the smaller amount of computation memory

required for RMO algorithm. This is because of the position and the velocity for most particles are not required to be moved between iterations. In addition, in performing RMO, the random transferring is searching for the global best blocks of the technique avoiding to be not located at global optimum [52]. The optimization process of RMO starts with propagating the particles throughout the search-space that gives the opportunity for suggesting the solution for the problems. The cost function in terms of objective function is estimated every step. The transferring of vector that is produced from particles generation located on the  $R_{best}$  (Radial Best),  $G_{best}$  (Global Best) and the random vector of particles. Like to DE and PSO algorithms, the particle position in search area is explained with  $(nPop * nDim)$  matrix. Where  $nPop$  denotes the particles amount, and  $nDim$  denotes the dimensions amount. The particles' number is usually selected based on the user. Whereas, the dimensions number depends on the variables number that required to be optimized. The preparing particles in the matrix are illustrated in (27) [52]. Fig. 16 illustrates the flowchart of the RMO technique.

$$x_{ij} = \begin{bmatrix} x_{1,1} & \dots & x_{1,nDim} \\ \vdots & \ddots & \vdots \\ x_{nPop,1} & \dots & x_{nPop,nDim} \end{bmatrix} \quad (27)$$

where  $i = 1; 2; 3; \dots; nPop$  and  $j = 1; 2; 3; \dots; nDim$

$$x_{ij} = Lb + r(Ub - Lb) \quad (28)$$

where  $Lb$  and  $Ub$  denote the lower and upper limits in search space and  $r$  denotes a random value.

The particles are dispersed in the form of a straight line from the center over the radius done according to the velocity vector  $V_{i,j}$  that obtained from (29).

**Step 1 Preparation. Recognize the optimization issue; chose several random fresh place of colonies**

**Step 2 Colonies Motion. Transfer the colonies on the way to their pertinent-imperialist**

**Step 3 Imperialist brings up to date. If the fresh colony has lesser cost in comparison with such of imperialist, interchange the position of such colony and the imperialist**

**Step 4 Imperialist Rivalry. Select the weakness colony from the most-weak empires and provide it to the empires, which has the utmost probability to possess it**

**Step 5 Carrying out. Reject the weak empires**

**Step 6 Bringing to an end norm control. Reiterate step 2-5 till the terminating norm is fulfilled**

Fig. 15. Pseudo code for imperialist competitive algorithm.

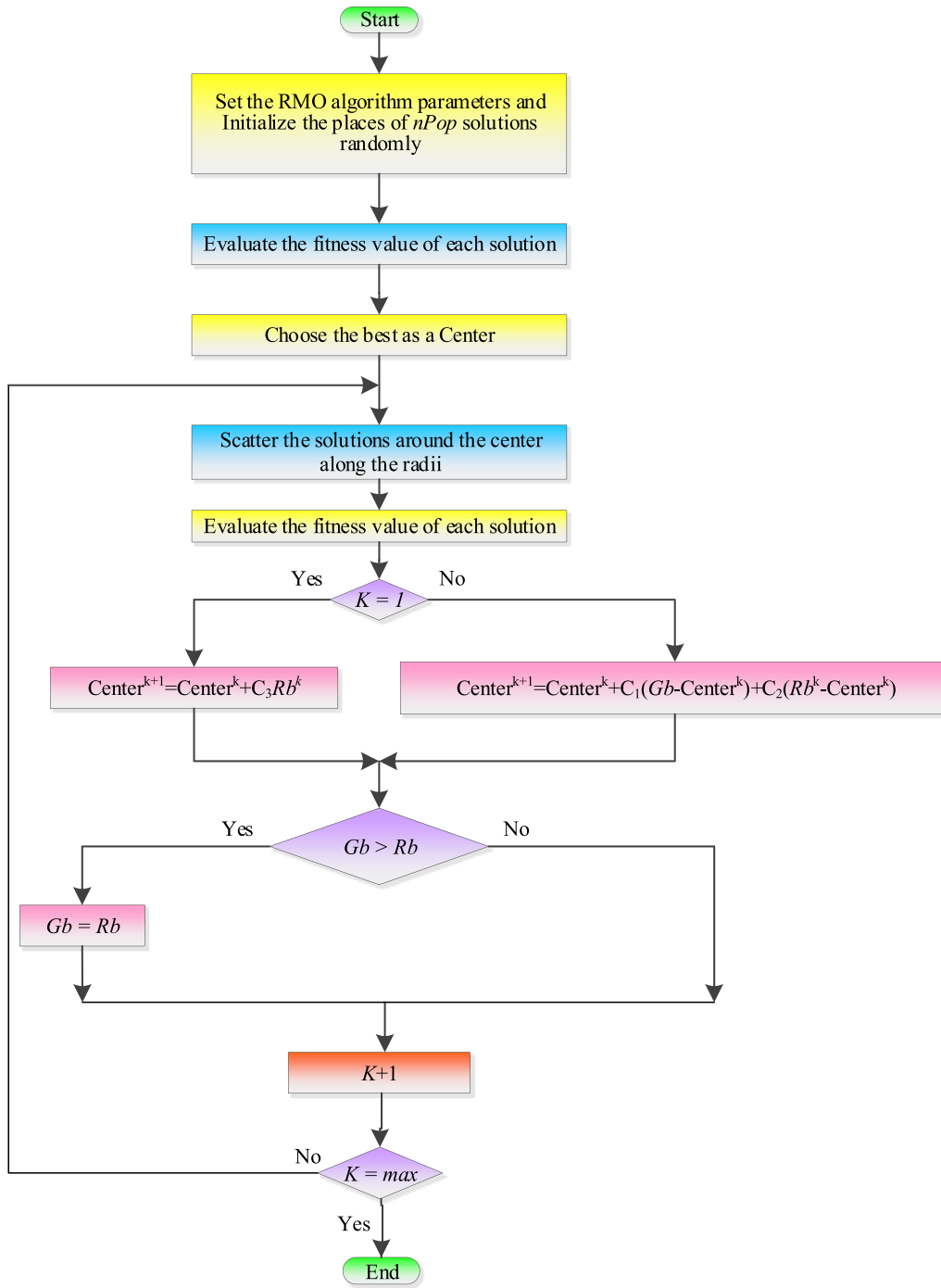


Fig. 16. Flowchart of radial movement algorithm.

$$V_{ij} = rV_{max(j)} \Rightarrow \begin{cases} V_{max(j)} = \frac{x_{max(j)} - x_{min(j)}}{k} \\ i = 1, 2, \dots, nPop \\ j = 1, 2, \dots, nDim \end{cases} \quad (29)$$

where  $X_{max(j)}$ ,  $X_{min(j)}$ : are the limits of  $j$ th dimension.

The inertia weight for RMO is represented with  $W$ , and it can be formulated by the following relation [132,134];

$$W_k = W_{max} - \left( \frac{W_{max} - W_{min}}{Iteration_{max}} \right) Iteration_k \quad (30)$$

where,  $W_{max}$ ,  $W_{min}$  denote the maximum and minimum values of the inertia weight and.

$Iteration_{max}$  is the maximum number of iterations.

$$V_{ij}^k = rW_k V_{max(j)} \quad (31)$$

The population is evaluated based on the fitness of each vector. The radial best ( $R_{best}$ ) vector is the particle that gives the minimum error of the current scattering swarm. The new center location is modified based on the following [78]:

$$Centre^{New} = Centre^{Old} + C_1 (G_{best} - Centre^{Old}) + C_2 (R_{best} - Centre^{Old}) \quad (32)$$

where  $C_1$  and  $C_2$  are two constants that affect  $R_{best}$  (Radial Best) and  $G_{best}$  (Global Best), respectively.

After the new center point has been obtained, the swarm is then re-scattered, and the process is repeated. The process of searching is

continued up until ending condition is reached.

### 3.13. Multi-verse optimizer (MVO)

MVO is deemed as one of the modern optimization methods that presented by Mirjalili, who inspired the concept of this technique from the multi-verse theory [135]. The theory of big bang discussed that the universe begins with a massive blast. Based on the theory, the source for everything in the world is a big bang. In general, the multi-verse theory is considered as famous and recent theory among physicists. This theory believed that there are more than one big bang and every big bang causes the universe birth [136,137]. There are three major concepts of multi-verse optimization algorithm motivation, white holes, wormholes, and black holes. White hole, as physicists assumed, is the prime of universe birth. The black hole has a large gravitational force, which leads to pull everything including the light. Moreover, the wormholes are responsible for linking the various parts of the universe together. The wormholes in the multi-verse theory behave as time or space travel tunnels in which the objects are fit to travel from one universe to another [138]. There are two phases of search space for MVO, exploration and exploitation. Both white and black holes are utilized for exploring the search spaces. On the other hand, the wormholes help MVO in exploiting the search spaces. The conceptual model of the multiverse technique is shown in Fig. 17.

The mathematical representation of MVO can be found in Refs. [136,137]. The universes are sorted related to their inflation rates and roulette wheel chooses one to have white holes in each trial. It can be represented as follows:

$$U = \begin{bmatrix} x_1^1 & \dots & x_1^d \\ \vdots & \vdots & \vdots \\ x_n^1 & \dots & x_n^d \end{bmatrix} \quad (33)$$

$$x_i^j = \begin{cases} x_k^j & r_1 < NI(U_i) \\ x_i^j & r_1 \geq NI(U_i) \end{cases} \quad (34)$$

where  $d$  is the number of variables to be determined,  $n$  denotes the number of universes,  $x_i^j$  is the  $j$ th object in the  $i$ th universe,  $NI(U_i)$  is the normalized inflation rate of universe  $i$ ,  $x_k^j$  is the  $j$ th object in the  $k$ th universe selected by roulette wheel mechanism and  $r_1$  is a random value.

After that, the objects in every universe attempt to move to the best universe throughout the wormholes, this process can be explained as follows:

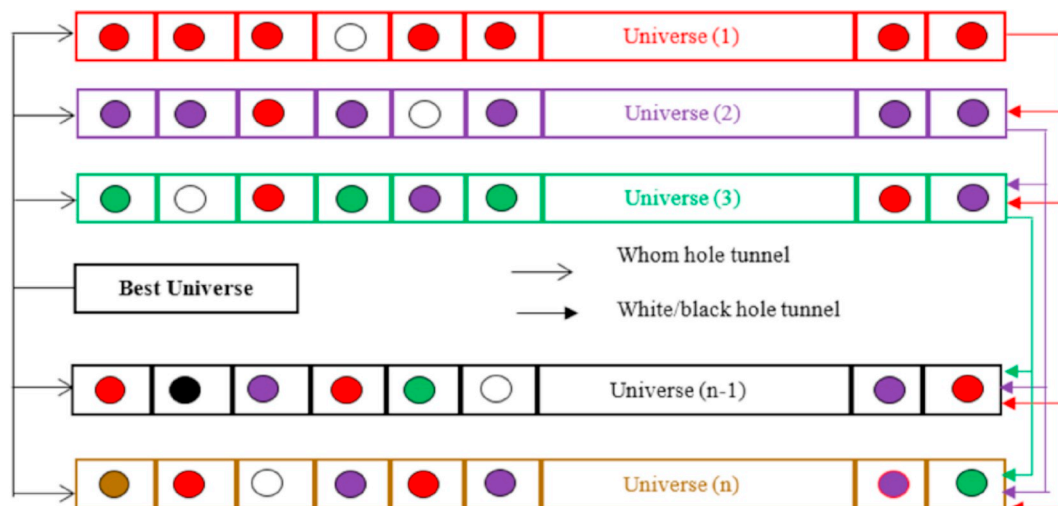


Fig. 17. Conceptual model for multi-verse optimization algorithm.

$$x_i^j = \begin{cases} X_j + TDR \cdot ((ub_j - lb_j) \cdot r_4 + lb_j) & r_3 < 0.5 \& r_2 < WEP \\ X_j - TDR \cdot ((ub_j - lb_j) \cdot r_4 + lb_j) & r_3 \geq 0.5 \& r_2 < WEP \\ x_i^j & r_2 \geq WEP \end{cases} \quad (35)$$

where  $X_j$  is the  $j$ th object in the best universe,  $ub_j$  and  $lb_j$  are the upper and lower limits of  $x_i^j$ ,  $r_2, r_3, r_4$  are random number in range between  $[0, 1]$ ,  $TDR$  is the rate of traveling distance rate, and  $WEP$  is the probability of wormholes existence [136,137]. The flowchart for MVO is shown in Fig. 18.

### 3.14. Whale optimization algorithm (WOA)

WOA is a recent heuristic optimization approach introduced by Mirjalili et al. [139]. It is motivated from the social behaviors of the strategy of whale in hunting process. The hunting process is named bubble-net feeding method, the favorite prey of the humpback whales is small fishes located near the water surface. The infectious prey process is performed through producing bubbles along a circle, these bubbles are classified into two categories; upward spiral and double-loops. In the first category, the humpback whale dives down about 12 m and then produces spiral shaped bubble around the prey, after that, it swims up to the surface. In the second jockey, three different stages are performed, coral loop, lob tail, and capture loop [139].

The humpback whales evaluate the current position of the prey. The position of the whale is updated until reaching the best search agent, the updating process can be expressed as follows:

$$\vec{X}^{k+1} = \vec{X}_p^k - \vec{A} \cdot \left| \vec{C} \cdot \vec{X}_p^k - \vec{X}^k \right| \quad (36)$$

where  $\vec{X}_p^k$  is the vector of prey position at iteration  $k$ ,  $\vec{X}^k$  is the position of the prey at iteration  $k$ ,  $\vec{A}$  and  $\vec{C}$  are coefficients determined by:

$$\vec{A} = 2\vec{a} \cdot r - \vec{a} \quad (37)$$

$$\vec{C} = 2 \cdot r \quad (38)$$

where  $\vec{a}$  is a vector decreased linearly from 2 to 0 and  $r$  is a random vector in the range  $[0, 1]$ . The attack process on the prey is performed via the bubble-net strategy or called exploration phase, the second phase followed in WOA is exploitation process in which two approaches are surveyed via humpback whales, mechanism of shrinking encircling and the spiral updating position. In the second approach, the distance between the position of whale and the prey is evaluated, based on this distance; the whale's position is updated in a spiral path to demolish the prey. The updating process is performed by the following eqn:

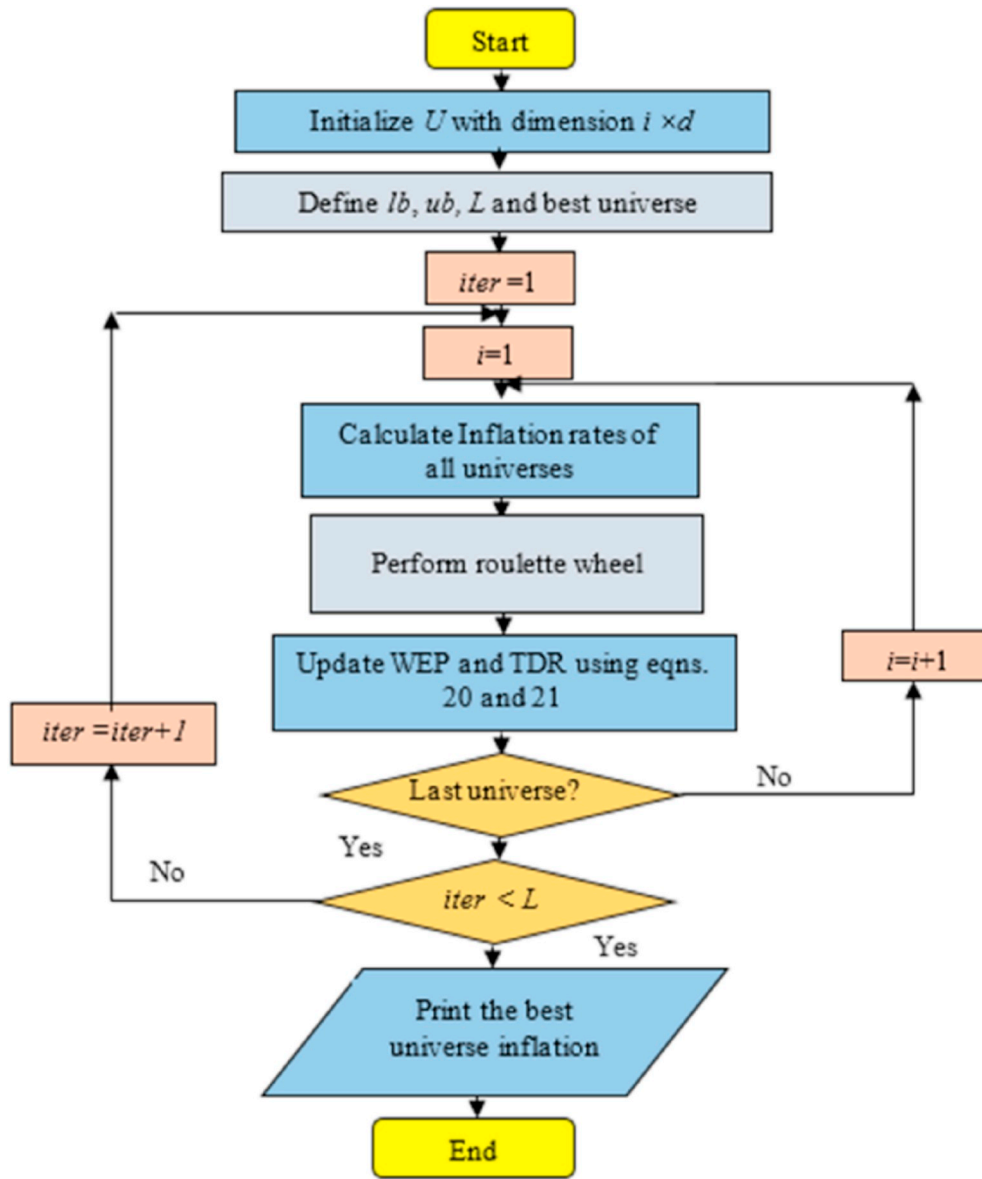


Fig. 18. Flowchart for multi-verse optimizer algorithm.

$$\vec{X}^{k+1} = \vec{X}_p^k + \left| \vec{X}_p^k - \vec{X}^k \right| \cdot e^{bl} \cdot \cos(2\pi l) \quad (39)$$

where  $b$  is a constant denotes the shape of logarithmic spiral,  $l$  is a random value in the range  $[-1, 1]$ . A probability index,  $Prob$ , is placed to discriminate between the two stated phases, in case of  $Prob$  less than 0.5, the first phase is taken place else the second one is executed.

The prey searching process is named exploration phase, this process is performed in a random manner, therefore, the vector  $\vec{A}$  is randomly selected greater than 1 or less than  $-1$  to oblige the search agent to move out of the reference whale. In case of selecting the vector  $\vec{A}$  greater than unity, the position is updated by:

$$\vec{X}^{k+1} = \vec{X}_{rand}^k - \vec{A} \cdot \left| \vec{C} \cdot \vec{X}_p^k - \vec{X}^k \right| \quad (40)$$

In WOA based MPPT, the design variable is duty cycle fed to the DC-DC converter while the objective function is the power extracted from the PV array.

### 3.15. Sine Cosine Algorithm (SCA)

Mirjalili presented an optimization approach named Sine Cosine Algorithm (SCA) [140]. The SCA algorithm produces a minor population and goes to the most suitable solution. For exploration and search area exploitation confirmation, the formulas of renew positions are written as follows [141]:

$$X_i^{t+1} = \begin{cases} X_i^t + r_1 \times \sin(r_2) \times |r_3 P_i^t - X_i^t| & r_4 < 0.5 \\ X_i^t + r_1 \times \cos(r_2) \times |r_3 P_i^t - X_i^t| & r_4 \geq 0.5 \end{cases} \quad (41)$$

where  $X_i^t$  is considered as the solution placement at iteration  $t$ . The parameters  $r_1, r_2, r_3$ , and  $r_4$  are random quantities that are ranged from 0 to 1. The  $P_i$  is the destination-placement. From eqn. (41), the parameter  $r_1$  indicates the subsequent placement areas that possibly will be located at the space within the solution and target or outgoing it. The parameter  $r_2$  describes how away the moving to be in the path of or away from the target. The parameter  $r_3$  provides random weights for gap point as a way to be randomly emphasized ( $r_3 > 1$ ), or de-emphasized ( $r_3 < 1$ ) in recognizing the space. The parameter  $r_4$  is considered as the switches between the sine and cosine additions. The

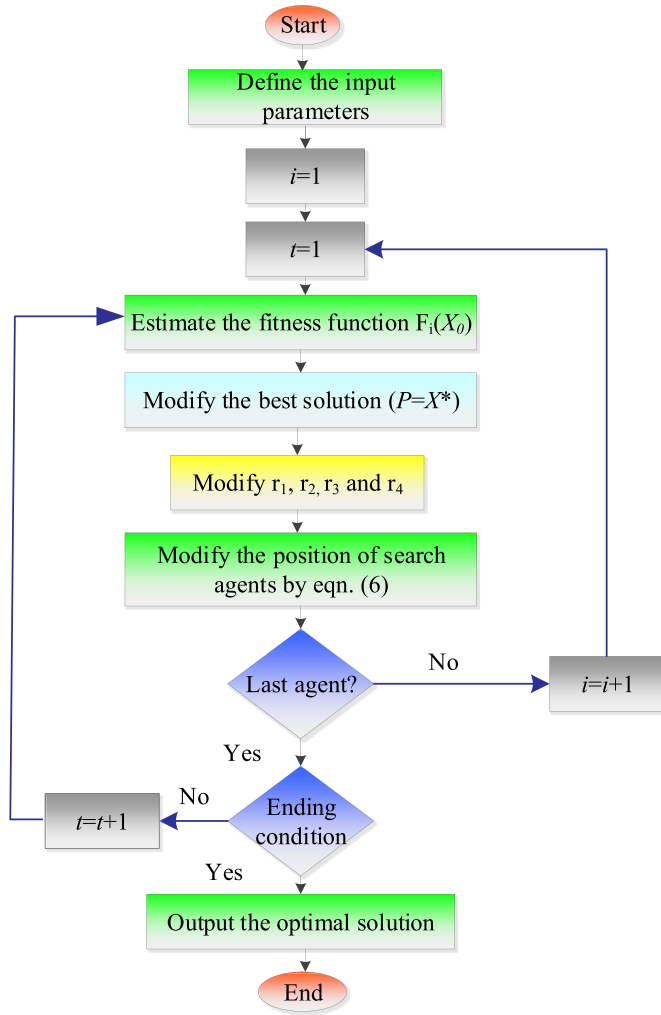


Fig. 19. The SCA main steps.

trajectory direction of the SCA population is given in Fig. 18. . The objective-function movements have to be towards the global optimum solution, and the algorithm utilizes the seeking area [140]. On the other hand, out of [-1, +1] range, the fitness characteristic moves away from the global optimum, and the technique explores the seeking area. According to converge the optimal global results, stabilizing operations among exploration and exploitation would be confirmed. Consequently, the sine and cosine variety is renewed adaptively using the following formula:

$$r_1 = a - t \frac{a}{T} \quad (42)$$

where  $a$  is a constant,  $t$  denotes current iteration and  $T$  denotes the total number of iterations. Fig. 9 shows the major operations of SCA.

The SCA based MPPT has been presented based on sensor for battery charging purpose. Additionally, it has been presented in a partially shaded condition of PV array via controlling the converter duty cycle.

### 3.16. Gravitational Search Algorithm (GSA)

Rashedi et al. [142] presented GSA; it has been motivated from the law of gravity [143]. In such approach, agents are taken into consideration as objects, and their overall performances are measured via their masses. Most of these items appeal to each different by the gravity force, and this force causes a global motion of all objects in the direction of the gadgets with heavier masses. For this reason, masses cooperate using right away the shape of conversation, through

gravitational force. The heavy masses, which correspond, to appropriate solutions flow more slowly than lighter ones, this ensures the exploitation step of the approach. Four items characterize each agent; position, mass, active, and passive gravitational masses. The mass positions are considered as problem solutions, while the objective function determines the others. By interval of time, it is expected that the masses will be attracted using the heaviest one which represents the best solution inside the search space.

Where  $G(t)$  is the gravitational constant at time  $t$ ,  $M_{aj}$  and  $M_{pi}$  are the active and passive gravitational masses of  $j$ th and  $i$ th agents,  $\varepsilon$  is tolerance and  $R_{ij}(t)$  is the Euclidian distance between  $i$ th and  $j$ th agents defined as follows:

$$R_{ij}(t) = \|X_i(t), X_j(t)\|^2 \quad (43)$$

The total force applied on  $i$ th agent can be expressed as follows:

$$F_i^d(k) = \sum rand_j F_{ij}^d(k) \quad j = 1, j \neq iN \sum \quad (44)$$

where  $rand_j$  is a random value in the range of [0, 1]. The agents' accelerations are calculated by dividing the total force on  $i$ th agent by the agent internal mass,

$$a_i^d(k) = \frac{F_i^d(k)}{M_{ii}(k)} \quad (45)$$

During the optimization process, the agents update their positions based on the updated velocities and current positions.

The GSA is considered as a remoted machine of masses. It is like a small synthetic international of loads obeying the Newtonian laws of gravitation and movement; law of gravity and law of motions. The first step in GSA is initializing  $N$ -dimension search agent as follows:

$$X_i = [x_i^1, x_i^2, \dots, x_i^d] \quad (46)$$

where  $N$  is the search agents' number,  $d$  is the problem dimension and  $x_i^d$  is  $i$ th agent in the  $d$ th dimension. During the implementation of GSA, there is mutual force between agent  $j$  on agent  $i$  at iteration  $t$  defined by:

$$F_{ij}^d(t) = G(t) \left( \frac{M_{pi}(t) \times M_{aj}(t)}{R_{ij}(t) + \varepsilon} \right) (x_j^d(t) - x_i^d(t)) \quad (47)$$

$$v_i^d(t+1) = rand_i \times v_i^d(t) + a_i^d(t) \quad (13)$$

$$x_i^d(t+1) = x_i^d(t) + v_i^d(t+1) \quad (14)$$

where  $rand_i$  is a random variable in the range [0, 1]. In GSA, the best agent has heavier mass with slow motion, the gravitational and internal masses can be updated as follows:

$$M_{ai} = M_{pi} = M_{ii} = M_i \quad i = 1, 2, \dots, N \quad (48)$$

$$m_i(t) = \frac{fit_i(t) - worst(t)}{best(t) - worst(t)} \quad (49)$$

$$M_i(t) = \frac{m_i(t)}{\sum_{i=1}^N m_i(t)} \quad (50)$$

where  $fit_i(t)$  is the  $i$ th agent fitness function at iteration  $t$ ,  $worst(t)$  and  $best(t)$  can be defined as follows:

$$\begin{aligned} best(t) &= \min_{j \in \{1, \dots, N\}} fit_j(t) \\ worst(t) &= \max_{j \in \{1, \dots, N\}} fit_j(t) \end{aligned} \quad (51)$$

The flowchart of GSA is given in Fig. 21(see Fig. 20). In GSA, three duty cycles are transmitted to the boost converter. These values serve as the best values for the first iteration. In the next iteration, the resulting mass is simplest due to the best and the worst values. This results in zero space and the duty cycle remain unchanged. A small perturbation in duty cycle is done. After that, all of the duty cycles reach the MPP.

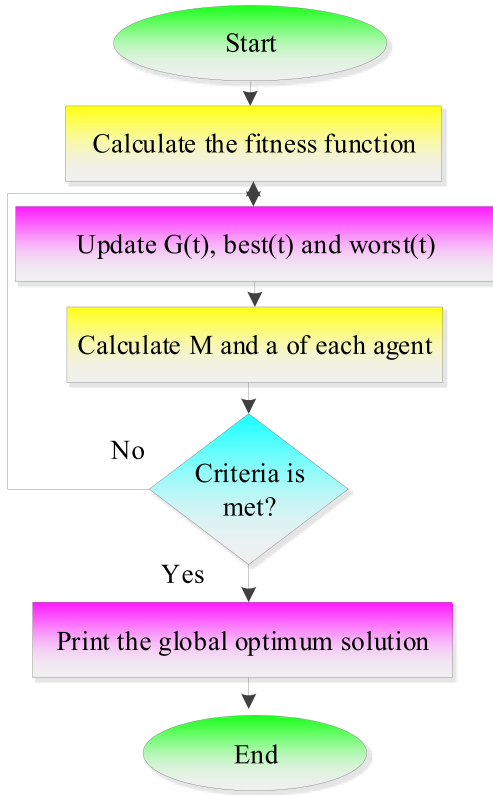


Fig. 20. GSA flowchart.

3.17. Cuckoo search (CS)

Cuckoo Search is executed depending on the proliferation plan of Cuckoo-Bird (CB) [144]. The numerous kinds of cuckoos (Cuc.) are executed by locating the CB eggs into the nest of steward-birds (SB) where they are hatching earlier. The SB will throughout the unfamiliar eggs once they are discovered or goes far from its position and rebuild a

new nest at another place. When the SB can't recognize the Cuc. eggs that are hatching a little bit once upon a time than the original-eggs, steward eggs, the hatched Cuc. eggs will reject the original-eggs from their place ensuring supplying food through the original-eggs. However, the suitable resolution of CS issue can be characterized by each egg in the nest, also a novel solution is introduced by cuckoo-egg, and the destination can be realized by taking out the most suitable new solutions for exchanging the unacceptable others in the nests. The main operation points of the CS optimizer are deduced as:

- I: **Preparation.** Introduce the primary nets;
- II: **Bring the Cuc. nets up to date.** Using updating formula, the novel solution  $x^{t+1}$  for  $i$  of CB can be formulated as [145]:

$$x_i^{t+1} = x_i^t + \alpha \oplus \text{Lévy}(\lambda) \tag{52}$$

where  $x_i^t$  represents the eggs at  $i$  egg number at  $t$  iteration and  $\alpha$  denotes step size ( $\alpha > 0$ ).

A Lévy distribution is represented as (53)

$$\text{Lévy}(\lambda) = t^{-\lambda} \tag{53}$$

where  $t$  denotes length of flight and  $\lambda$  denotes the variance.

A simplified scheme of the Lévy distribution is formulated as (54) according to Mantegna's algorithm [101]:

$$s = \alpha_0(x_{best} - x_i) \oplus \text{Lévy}(\lambda) \simeq K \left( \frac{u}{|v|^{1/\beta}} \right) (x_{best} - x_i) \tag{54}$$

where  $\beta$  is equal to 1.5,  $\alpha_0$  denotes the initial step change,  $K$  is the multiplying factor of Lévy,  $u$  and  $v$  denote random values as in (55)

$$u \approx N(0, \sigma_u^2); v \approx N(0, \sigma_v^2) \tag{55}$$

The  $\sigma_u$  and  $\sigma_v$  are variables formulated as follows:

$$\sigma_u = \left[ \frac{\Gamma(1 + \beta) \times \sin(\pi \times \beta/2)}{\Gamma((1 + \beta)/2) \times \beta \times 2^{(\beta-1)/2}} \right]^{1/\beta}; \text{ and } \sigma_v = 1 \tag{56}$$

where  $\Gamma$  denotes the integral gamma function.

According to the issue of MPPT, the iterations will be stopped in the case of all samples find the last MPP. In Ref. [51], CS via MPPT is implemented. The produced voltage of the PV system can be considered

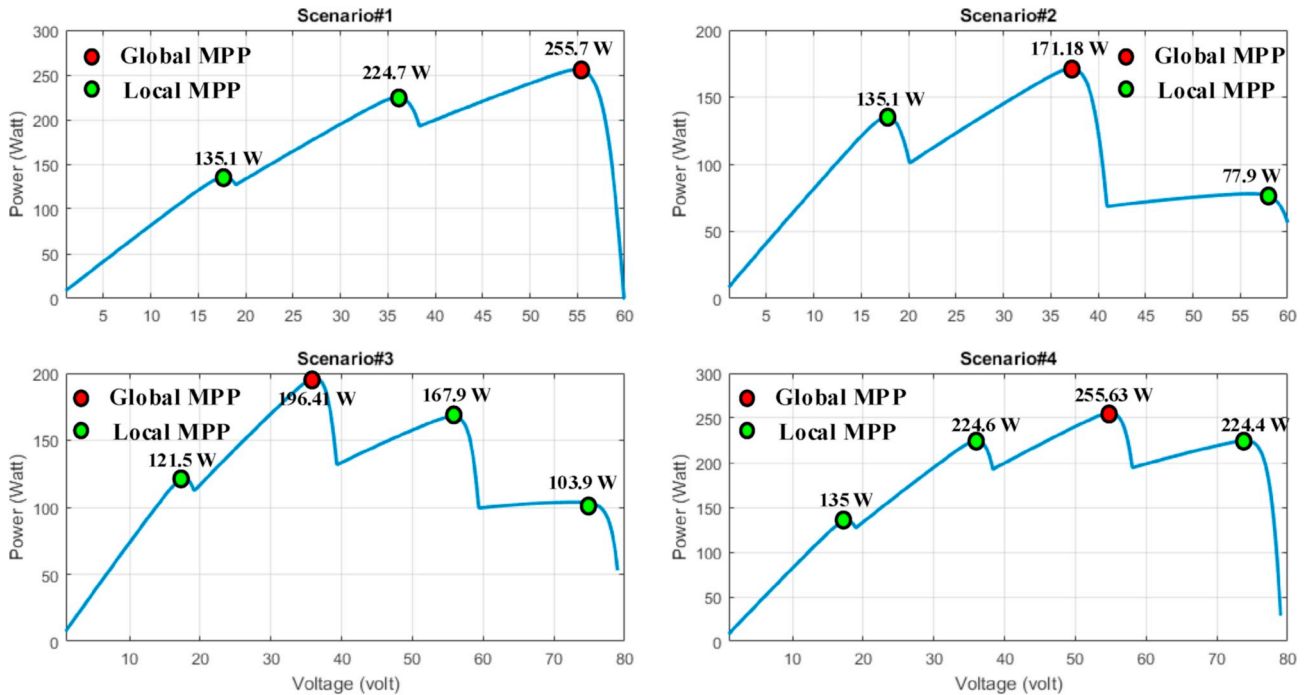


Fig. 21. The voltage against power curves of PV system with different shadowing scenarios.

as samples. The produced power of PV panels can be represented as fitness function. The performance of the CS via MPPT is constructed using an emulation scheme via buck-boost converter. The results confirmed that, CS is superior and fast with high performance as compared with P&O and PSO.

### 3.18. Firefly optimization algorithm (FA)

FA is based on the behavior and flashing of fireflies [146,147]. It has three major presumptions. First of all, any firefly will be attracted to the brighter one. In the second presumption, based on the space between fireflies itself and any other fly, the attractive one is referred to its brightness. Lastly, given fireflies will move randomly in the case of there is no brighter one. Therefore, for a given issue, the brightness of firefly can be considered as the objective function. The basic steps of FA are performed in the following steps:

- **I: Initialization.** Initialize the population of fireflies,  $x_i$ , Determine the corresponding fitness function,
- **II: Determine brightness/assimilation coefficient (Update function).** According to the increase in the distance between two flies, the attractiveness decreases because of the light absorption in air. FA uses the exponential decay through a medium rather instead of using the inverse-square law regarding to distance from the source. The attractiveness (or brightness),  $\beta$ , of each firefly can be written as follows:

$$\beta(r) = \beta_0 \exp(-\gamma r^m), m \geq 1 \tag{57}$$

where the space between fireflies is represented by  $r$ ,  $\beta_0$  is the primary attraction at zero distance,  $\gamma$  is an assimilation coefficient and  $m$  is a constant. The target of the assimilation coefficient is to control the mitigation of the strength of the light. Eqn. (7) introduces the Euclidean distance between fireflies  $i$  and  $j$  at placements  $x_i, x_j$  as follows:

$$r_{ij} = \|x_i - x_j\| = \sqrt{\sum_{k=1}^d (x_{i,k} - x_{j,k})^2} \tag{58}$$

where  $d$  is the dimension of a given issue and  $x_{i,k}$  ( $x_{j,k}$ ) can be considered as the locative coordinates of  $k$ th component of  $i$ th ( $j$ th) firefly.

- **III: Attracted fireflies.** The fireflies that have lower brightness are moved towards, thus attracted, brighter one. The movement of firefly is formulated as:

$$x_i^{k+1} = x_i^k + \beta_0 \exp(-\gamma r_{ij}^m)(x_j^k - x_i^k) + \alpha(randn - 0.5) \tag{59}$$

where  $randn$  is the random number and  $\alpha$  is the motion factor considered random values ( $\alpha \in [0, 1]$ ). After the motion, the value of fitness of the novel placements are determined and the strengths of the light are updated.

- **IV: The superior solution.** In accordance to all fireflies are moved, they should be arranged, and detect the superior solution;
- **V: End.** When the ending condition is achieved. Else, boost the nest iteration and start from III.

According to Ref. [85], FA was satisfied to PV system for MPPT under PSC. In this situation, the  $d$  in eqn. (58) is equal to unity.

In the standard FA, each comparison between each firefly outcomes a series step of moving toward the attracted fireflies. Nevertheless, the tortuous path of a huge number of attracted flies cause an exceedingly long tracking time via very complicated computation. To overcome this issue, a modified FA (MFA) is implemented in Ref. [86]. The MFA considers the median of all attracted fireflies that are considered as strength point. In this regard, the firefly is going to such point. According to that, the updating eqn. (59) is renewed where the  $r_{ij}$  is changed to  $r_{ij, avg}$  as follows [86]:

$$x_i^{k+1} = x_i^k + \beta_0 \exp(-\gamma r_{ij, avg}^m)(x_j^k - x_i^k) + \alpha(randn - 0.5) \tag{60}$$

The median coordinate of the attracted fireflies can be written as:

$$x_{j, avg} = \frac{1}{L} \sum_{m=1}^L x_j \tag{61}$$

where  $L$  is the total of attracted flies. Consequently,  $x_i$  is updated according to the median of all the attracted flies that decreases the amount of evaluation time and increases the acceleration of search operation. The results of the simulation scheme illustrated that, the MFA has been very effective with high performance to track the global MPP.

### 3.19. Genetic algorithm (GA)

GA is created on the basis of the operation of the natural-part in the theoretical determination of Darwin. GA is prepared to deduce the most suitable results to the nonlinearity of the several issues of optimizers. Each solution is decoded as a binary matrix that defined in terms of chromosome. The quality of these agents, population solution, is raised bringing their amounts of fitness up to date. The major operation points of GA can be deduced from Refs. [148,149].

Actually, GA is regularly not immediately applied to the MPPT issue due to its low speed to track the MPP. As an alternative, GA is utilized to be optimized other global MPP techniques to track the MPP very fast with high accuracy as follows. In Ref. [87], depending on the MPPT, fuzzy logic control (FLC) parameters optimized by GA. In the same way, the GA is executed to train the artificial neural network (ANN) for predicting the optimum voltage and current at the MPP of PV array [88]. Moreover, GA has been implemented to be stratified in the economic design of PV array with various inverters [89]. This work has been produced by realizing the net present value (objective-function) and the adjusted electric restrictions as the restrictions of GA.

### 3.20. Jaya Algorithm (JA)

JA is inspired by victory i.e. the act of overcoming the contender enemy in a battle or competition or driving out the hindrance from the craved way [150]. JA only necessitates the joint dominance parameters to detect the most suitable solution staying away from the worst. The JA always try to be victorious by detecting the most suitable solution and refuse the worst (**Jaya** means **victory**). JA works only in one phase to get the optimal solution. JA can be considered as a superior technique to be applied for the MPPT of PV systems, due to the fact that JA is simple to be constructed, flexible, fast, and has high performance. A stepwise operation of JA can be given as [150]:

- **I: Initialization.** Initialize the population size ( $ps = 1, 2, \dots, nc$ ) where  $nc$  is the number of candidate solutions, designing elements number ( $de$ ), and  $s$  iteration numbers;  $f(x)$  is the fitness function (objective);
- **II: Evaluation.** Evaluate the different values of  $f(x)$  in the entire candidate solutions;
- **III: Update (Modify) solution.** Assuming the random variables ( $r_1$  and  $r_2$ ) within the range  $[0:1]$ , the design variables value are renewed based on the following formula:

$$X'_{j,s,i} = X_{j,s,i} + r_{1,j,i}(X_{j,best,i} - |X_{j,s,i}|) - r_{1,j,i}(X_{j,worst,i} - |X_{j,s,i}|) \tag{62}$$

where,  $X_{j,best,i}$  and  $X_{j,worst,i}$  are the values of factor  $j$  for the most suitable (*best*) and worse solutions respectively. The term  $r_{1,j,i}(|X_{j,best,i} - |X_{j,s,i}||)$  and  $r_{2,j,i}(|X_{j,worst,i} - |X_{j,s,i}||)$  specify the inclination of the solutions to go near to the most suitable one and avert the worse one respectively.  $X'_{j,s,i}$  indicates the updated result of  $X_{j,s,i}$  and it considered as acceptable with better results;

- **IV:** All the acceptable results at the ending of the iteration are

**Table 2**  
The update equations and the tuning parameters for deferent optimizers.

Optimizer	Update equation for step size	Tuning parameters
<b>Particle swarm optimization</b>	$O_i^{k+1} = wO_i^k + k_1 r_1 \{b_{bi} - X_i^k\} + k_2 r_2 \{G_b - X_i^k\}$	$k_1, k_2$ : coefficient of acceleration $w$ : inertia weight $r_1, r_2$ : random value between 0 and 1 $P_{best}$ : local best $G_{best}$ : global best $r_1$ and $r_2$ : randoms
<b>Differential Evolution</b>	$dv_i = D_{best} + F \times (d_{r1} - d_{r2})$	$F$ : scaling factor $d_{r1}, d_{r2}$ : two vectors chosen randomly between population $D_{best}$ : the best value of duty cycle
<b>Flower Pollination</b>	$x_i^{t+1} = x_i^t + \gamma L(\lambda)(g_s - x_i^t)$	$x_i^{t+1}$ : pollen for same kind of flower at iteration $t$ $g$ : the best value of duty cycle $\gamma$ : scaling factor $L(\lambda)$ : Lévy flights
<b>Teaching-learning-based optimization</b>	$diff_{mean\ i} = r_i * (M_{new} + T_f * M_i)$	$M_i$ : mean rate of learners $M_{new}$ : new mean rate of learners $r_i$ : random number between [0,1] $diff_{mean\ i}$ : difference between the present and desirable mean $T_f$ : teacher factor that may equal 1 or 2
<b>Grey wolf optimization</b>	$\vec{D} =  \vec{C} \cdot \vec{X}_p(t) - \vec{X}(t)  \vec{X}(t+1) = \vec{X}_p(t) - \vec{A} \cdot (\vec{D})$	$t$ : is the current position $\vec{X}_p$ : the position vector of prey $\vec{X}$ : the position vector of grey wolves $\vec{A}$ and $\vec{C}$ indicate the coefficient vectors
<b>Water cycle algorithm</b>	$x_{Stream}^{t+1} = x_{Stream}^t + r \text{ and } C \times (x_{River}^t - x_{Stream}^t) x_{River}^{t+1} = x_{River}^t + rand \times C \times (x_{Sea}^t - x_{River}^t)$	$x_{Stream}^t, x_{River}^t$ and $x_{Sea}^t$ : a: the positions of streams, rivers and sea at iteration number $t$ , $rand$ : random value $C$ : constant value $\alpha$ : reduction constant
<b>Mine blast algorithm</b>	$V_j^k = \frac{V_j - 1}{\exp\left(\frac{k}{\alpha}\right)}$	$V_j^k$ : indicated the distance pf produced shrapnel pieces for each iteration $k$
<b>Dragonfly Algorithm</b>	$\Delta X_i(k+1) = sS_i(k) + aA_i(k) + cC_i(k) + fF_i(k) + eE_i(k) + \omega \Delta X_i(k) X_i(k+1) = X_i(k) + \Delta X_i(k+1)$	$X$ and $\Delta X$ : the location and step vector of a search agent at iteration $k$ $\omega$ : is the inertia weight $S_i, A_i, C_i, F_i$ , and $E_i$ : the behaviors fitness values of search agent $i$ $\omega, a, c, f$ , and $e$ : the weights of the behaviors
<b>Antlions optimizer</b>	$Ant_v^k = \frac{R_A^k + R_E^k}{2}$	$R_A^k$ : denote the random walk beside the antlions $R_E^k$ : denote the random walks around elite at iteration $i$ .
<b>Imperialist Competitive Algorithm</b>	$x^{k+1} = x^k + \gamma \cdot \delta \cdot d$	$x^{k+1}$ : new position $x^k$ : position at iteration $k$ $\gamma$ : assimilation coefficient $\delta$ : random $d$ : distance between colony and its imperialist.
<b>Radial movement optimization</b>	$Centre^{New} = Centre^{Old} + C_1(G_{best} - Center^{Old}) + C_2(R_{best} - Center^{Old})$	$C_1$ and $C_2$ are two coefficients $R_{best}$ : Radial Best $G_{best}$ : Global Best $Centre^{Old}$ : old value of center
<b>Multi-verse optimizer</b>	$x_i^j = \begin{cases} X_j + TDR \cdot ((ub_j - lb_j) \cdot r_4 + lb_j) & r_3 < 0.5 \text{ \& } r_2 < WEP \\ X_j - TDR \cdot ((ub_j - lb_j) \cdot r_4 + lb_j) & r_3 \geq 0.5 \text{ \& } r_2 < WEP \\ x_i^j & r_2 \geq WEP \end{cases}$	$X_j$ : the $j$ th object in the best universe $ub_j$ and $lb_j$ : upper and lower bound $r_2, r_3, r_4$ : random values $TDR$ : traveling distance rate $WEP$ : probability of worm holes in the universes confirming the exploitation.
<b>Slap swarm algorithm</b>	$X_j^1 = \begin{cases} F_j + r_1((ub_j - lb_j)r_2 + lb_j), & r_3 \geq 0 \\ F_j + r_1((ub_j - lb_j)r_2 + lb_j), & r_3 < 0 \end{cases}$	$X_j^1$ : is the position of the leader in the $j$ -th dimension $F_j$ : is the place of food source in the $j$ -th dimension $ub_j, lb_j$ : are the upper an and lower bound of $j$ -th dimension receptivity $r_1, r_2$ , and $r_3$ are random number
<b>The whale optimization algorithm</b>	$\vec{X}^{k+1} = \vec{X}_p^k - \vec{A} \cdot \left  \vec{C} \cdot \vec{X}_p^k - \vec{X}^k \right $	$\vec{X}_p^k$ : vector of prey position at iteration $k$ $\vec{X}^k$ : position of the prey at iteration $k$ $\vec{A}$ and $\vec{C}$ : coefficients
<b>Sine Cosine Algorithm (SCA)</b>	$X_i^{t+1} = \begin{cases} X_i^t + r_1 \times \sin(r_2) \times  r_3 P_i^t - X_i^t  & r_4 < 0.5 \\ X_i^t + r_1 \times \cos(r_2) \times  r_3 P_i^t - X_i^t  & r_4 \geq 0.5 \end{cases}$	$X_i^t$ : the current solution position at iteration $t$ $r_1, r_2, r_3$ and $r_4$ : random values $P_i$ : the destination point position.
<b>Gravitational Search Algorithm</b>	$v_i^d(t+1) = r \text{ and } i \times v_i^d(t) + a_i^d(t) x_i^d(t+1) = x_i^d(t) + v_i^d(t+1)$	$x_i^d(t)$ : the position of $i$ th agent in $d$ -dimensional search space at iteration $t$ $v_i^d(t)$ : the velocity of $i$ th agent in $d$ -dimensional

(continued on next page)

Table 2 (continued)

Optimizer	Update equation for step size	Tuning parameters
Cuckoo search	$x_i^{t+1} = x_i^t + \alpha \oplus \text{Lévy}(\lambda)$	search space at iteration $t$ $rand_i$ : a random variable in range [0, 1]. $x_i^{t+1}$ : new solution for cuckoo bird $i$ ; $x_i^t$ : is the samples (eggs); $\alpha$ : is the step size and is $> 0$ ; $\oplus$ : refers to entry-wise multiplication; $\text{Lévy}(\lambda)$ : is a simplified Lévy distribution.
Firefly algorithm	$x_i^{k+1} = x_i^k + \beta_0 \exp(-\gamma r_{ij}^m)(x_j^k - x_i^k) + \alpha(randn - 0.5)$	$x_i, x_j$ : are the positions of fireflies between two flies $i$ and $j$ ; $k$ : is the iteration number; $\beta_0$ : is the primary attraction at zero "r" distance; $\gamma$ : is presented as an assimilation coefficient managing the decreasing of the light strength; $m$ : is a constant; $randn$ : is random number; $\alpha$ : is the motion factor considered random values within range (0: 1). $p_i$ : probability of selecting the of fitness proportionate selection; $f_i$ : is the fitness of an individual $i$ ; $N_{ind}$ : individuals.
Genetic Algorithm	$P_i = \frac{f_i}{\sum_{j=1}^{N_{ind}} f_j}$	$X_{j,best,i}$ : is the most suitable selection of the variable $j$ ; $X_{j,worst,i}$ : is the worse selection; $X_{j,s,i}$ : considers the updating of $X_{j,s,i}$ ; $r_1$ and $r_2$ : are random values.
Jaya Algorithm	$X'_{j,s,i} = X_{j,s,i} + r_{1,j,i}(X_{j,best,i} -  X_{j,s,i} ) - r_{1,j,i}(X_{j,worst,i} -  X_{j,s,i} )$	

Table 3  
PV module specifications.

Maximum power, $P_{max}$	135 W
Open circuit voltage, $V_{oc}$	22.1 V
Short circuit current, $I_{sc}$	9.37 A
Temperature coefficient of current, $k_i$	$5.02e^{-3} \text{ A}/^\circ\text{C}$
Temperature coefficient of voltage, $k_v$	$-8e^{-2} \text{ V}/^\circ\text{C}$
Reference temperature, $T_{ref}$	$25^\circ\text{C}$

Table 4  
The voltage, current and power of PV system with different shading scenarios.

Scenario	Solar irradiance Levels ( $\text{W}/\text{m}^2$ )	Voltage at MPP, V	Current at MPP, A	Power at MPP, W	Position of GMPP
1	100,800,600	54.90	4.66	255.70	Right
2	100,600,200	37.14	4.61	171.18	Center
3	900,700,400,200	36.26	5.42	196.41	2 <sup>nd</sup> left
4	1000,800,600,400	54.91	4.66	255.636	2 <sup>nd</sup> right

preserved, and these results are represented as the input to the next iteration. In this regard,  $f(x)$  is estimated and compared with the previous values and it is updated via values of designing factors at the ending of  $i$ -th iteration depending on their fitness.

- **V: Selection.** After updating  $f(x)$ , the most suitable and worse solutions are elected. For the next iteration, the most suitable and worse selection are considered. Thus, after the selection of the novel values for random variables, the designing factors are renewed according to III and IV.
- **VI: End.** When the stopping condition is achieved. Else boost the operation and repeat again from III.

In JA technique, the updating of the selected solutions can be managed by random values  $r_1$  and  $r_2$  to confirm perfect exploration of the solution space. Whatever this random operation is not enough to assure perfect MPPT for PV schemes. To overcome this problem and increase such attitude from the point of view of effectiveness, rapid

concourse and inferior fluctuation, natural cubic spline (NCS) depending on PV power output prognosis scheme has been combined into the iterative solution renew of the JA that named NCS S-Jaya by Ref. [90]. The employing of the NCS scheme in the iterative operation of the S-Jaya can avert the worst updates reducing negative solutions via improving the attitude of the MPPT. At the same time, the NCS scheme can be renewed online to keep its prognosis precision and deduce right decisions of novel solutions.

Based on section three, it can be said that the main difference between the optimizers are the updating equation of step size and the number of tuning parameters. Accordingly, Table 2 summarizes the update equations and the tuning parameters for different optimizers.

#### 4. Results and discussion

The PV system that studied in this research consists of PV array, DC-DC boost converter, and battery bank of 120 V. The parameters of the converter are 1 mH, 47  $\mu\text{F}$  and 47  $\mu\text{F}$  for the input inductance, input capacitor, and output capacitor respectively. The sampling time of MPPT is 0.01 s. The specifications of the solar panel are tabulated in Table 3.

A comprehensive comparison through an extensive statistical analysis of different considered algorithms is carried out. For evaluating and testing the performance of considered optimizers, each algorithm had been executed 50 times. Four different shading scenarios have been investigated. Change shading scenario is used to transfer the position of the global peak from left to right or middle for measuring the response of every algorithm with different conditions. Table 4 and Fig. 21 show the details of the considered scenarios. Two different PV systems have been studied. The first system (3SPVS) comprises three solar panel series connected and the other system (4SPVS) includes four series-connected solar panels. The first and second shading patterns were used with 3SPVS, whereas the third and fourth patterns were used with 4SPVS. The intensities of the solar radiation are 1000, 800, 600  $\text{W}/\text{m}^2$  for first, second, and third PV panels, respectively, in the first shading pattern. For this case, there are three MPPs. The global peak of 225.7 W

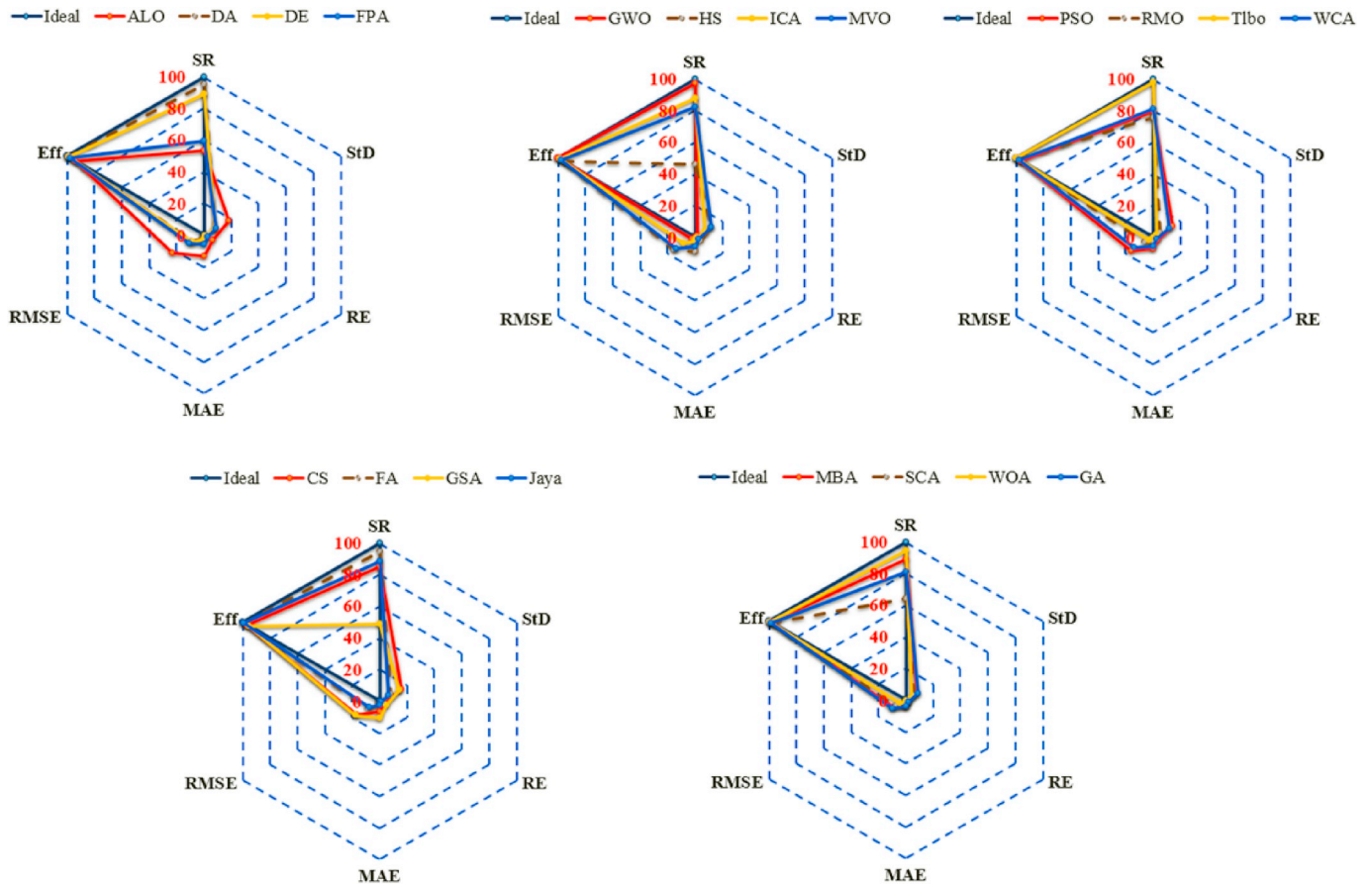


Fig. 22. Comparison among various algorithms and ideal case according to six statistical metrics.

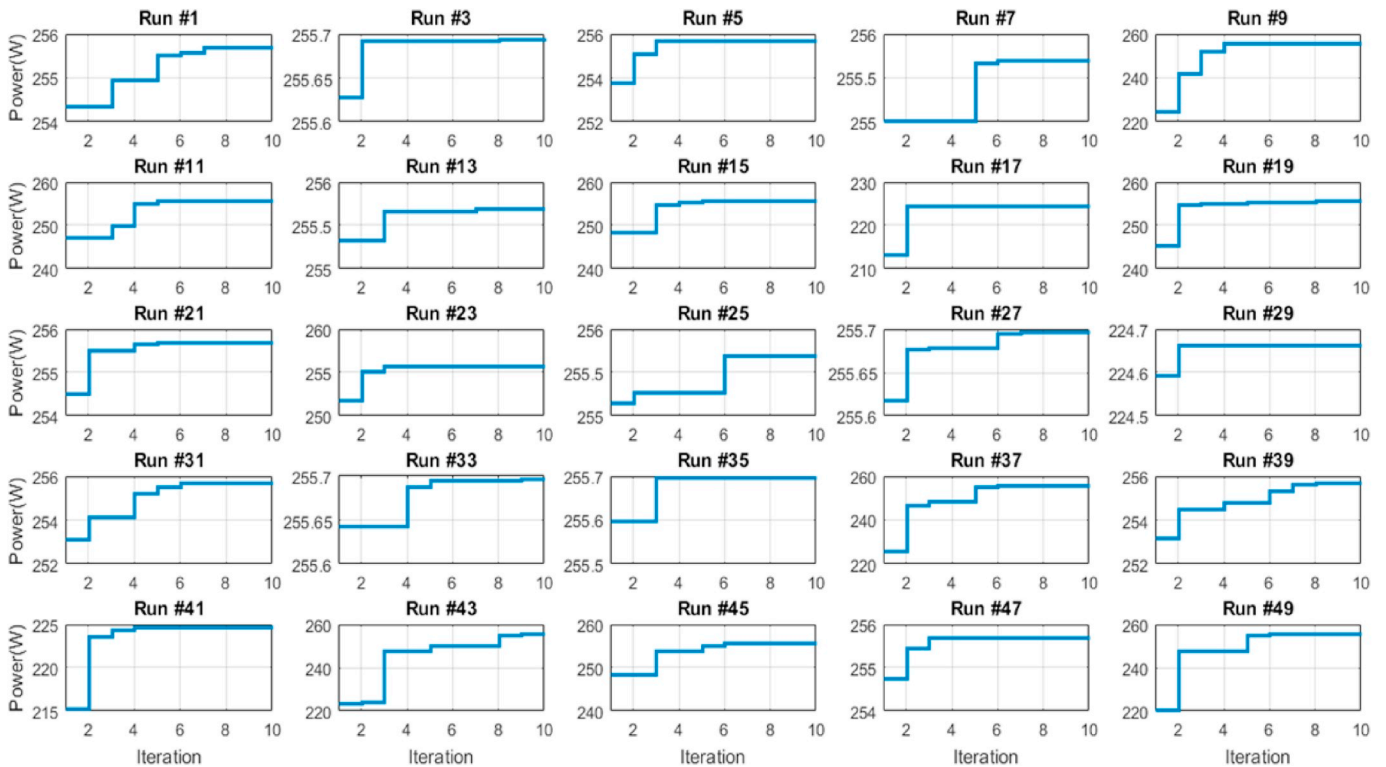


Fig. 23. The cost function variation for TLBO (the best optimizer) in case of first PSC scenario for each run.

is located at the right of the power-voltage curve. The details of other shading patterns are illustrated in Fig. 21.

A descriptive statistical analysis is introduced to evaluate, organize, and summarize the results obtained from the proposed algorithms. Moreover, sensitivity analysis is introduced to test the performance stability of these algorithms. The worthy six statistical metrics for this evaluation are, Relative Error (RE), Root Mean Square Error (RMSE), Mean Absolute Error (MAE), Standard Deviation (StD), Successful Rate (Suc.Rate), and efficiency. These metrics can be estimated as follows:

$$RE = \frac{\sum_{i=1}^{n_r} (P_{PVe,i} - P_{pvt})}{P_{pvt}} * 100\% \tag{38}$$

$$MAE = \frac{\sum_{i=1}^{n_r} (P_{PVe,i} - P_{pvt})}{n_r} \tag{39}$$

$$RMSE = \sqrt{\frac{\sum_{i=1}^{n_r} (P_{PVe,i} - P_{pvt})^2}{n_r}} \tag{40}$$

$$StD = \sqrt{\frac{\sum_{i=1}^{n_r} (P_{pvt} - \bar{P}_{pvt})^2}{n_r}} \tag{41}$$

Where  $n_r$  represents the no. of runs of the SIMULINK model. The successful rate (Suc.Rate) is identified as the fraction of no. of achieving the correct global peak into summation of iterations. To analyze and evaluate the performance of each considered algorithm, the general parameters are unified; population size = 5, no. of iterations = 10, and no. of executions for every optimizer algorithm = 50. The specific input parameters for every algorithm are displayed in Appendix A (Table A1). Table A2 illustrates the statistical performance evaluation for every algorithm with changing shading scenarios.

A comparison among various considered algorithms and ideal case according to six statistical metrics are shown in Table A3 in Appendix A and Fig. 22. Based on this comparison, it can be concluded that, TLBO and GWO have higher success rate of 98% and 97% respectively. On contrary, HS and GSA have the lowest SR of 46% and 49% respectively. The StD changes between 2.05 and 18.3. The biggest value for ALO optimizer and the smallest for GWO. TLBO has a good level of StD of

2.96 in comparison of with other optimizers. The relative error level is very small in case of TLBO and GWO not more than 0.3 in both. RMSE is ranged between 2.13 and 22.69. The lowest value for ALO optimizer. Regarding the tracking efficiency, most of the optimizers have an efficacy greater than 95% except ALO has 93.6%. TLBO has the highest efficiency rate of 99.75% followed by GWO. Ultimate, it can be concluded that GWO and TLBO are the top algorithms compared with the others. ALO has the lowest performance.

The detailed performance of every algorithm for the first PSC scenario are shown in Table A4 in Appendix A. The cost function variation for TLBO algorithm in case of first shading scenario for each run is depicted in Fig. 23.

### 5. Conclusion

This paper presents a review on the state-of-the-art global maximum power point tracking (MPPT) techniques based on modern optimization algorithms for PV system under shadowing condition. These algorithms have been surveyed, and their advantages and disadvantages were compared based on extensive statistical analysis. Six statistical metrics are employed to evaluate the performance of considered algorithms. According to this comparison, it can be seen that TLBO and GWO have the highest success rate of 98% and 97% respectively. On contrary, HS and GSA have the lowest SR of 46% and 49% respectively. The StD varies between 2.05 and 18.3. The biggest value is obtained via ALO optimizer and the smallest one is due to GWO. TLBO has a good level of StD of 2.96 in comparison of with other optimizers. The relative error level is very small in case of TLBO and GWO not more than 0.3 in both. RMSE is ranged between 2.13 and 22.69, the lowest value for ALO optimizer. Regarding to the tracking efficiency, most of the studied optimizers have efficiency higher than 95% except ALO has 93.6%. TLBO has the highest efficiency rate of 99.75% followed by GWO. Ultimate, it can be concluded that, GWO and TLBO are the best optimizers compared with the others while ALO has the lowest performance. This study is expected to provide very beneficial tool to all the researchers working on the PV system and to all the industries excelled in generating efficient, clean and sustainable energy to the humankind.

### Appendix A

Table A1  
input parameters for each optimizer

FPA		DE		
Probability switch	0.7	$F$	mutation ratio	0.6
beta	1.5	CR	crossover ratio	0.67
TLBO		CS		
Teaching Factor	randi([12])	$\beta$	beta factor	1.5
$r_1$	random value	$k$	Multiplying factor	0.1
ICA		GA		
Assimilation Coefficient	1.5	Crossover Percentage		0.8
Revolution Probability	0.05	Mutation Percentage		0.1
Revolution Rate	0.1	PSO		
Colonies Mean Cost Coefficient	0.2	$w$	inertia weight	0.4
SCA		$r_2$	random value	[0 1]
$a$	constant	$r_3$	random value	[0 1]
$r_2$	random value	$k_1$	coefficient of acceleration	1
$r_3$	random value	$k_2$	coefficient of acceleration	1
$r_4$	random value	GWO		
HAS		$i$	number of iteration	
number of new harmonics	5	Mc	variable	0.1-0.02i
Harmony Memory Consideration Rate	0.9	$S$	Separation weight	2*rand*Mc
Pitch Adjustment Rate	0.1	$A$	Alignment weight	2*rand*Mc
Fret Width Damp Ratio	0.995	$C$	Cohesion weight	2*rand*Mc
MBA		$F$	Food attraction weight	2*ran
Reduction factor	0.8	$E$	Enemy distraction weight	Mc
RMO		SCA		
Global Learning Coefficient	0.7	$r_2$	random value	(2*pi)*rand()
Personal Learning Coefficient	0.8	$r_3$	random value	2*rand

Table A2  
Output performance of considered algorithms under different shading scenarios

Algorithm	ALO	DA	DE	FPA	GWO	HS	ICA	MVO	PSO	RMO	Tlbo	WCA	CS	FA	GSA	Jaya	MBA	SCA	WOA	GA
Success rate (SR)																				
Scenario 1	48	96	88	62	96	42	84	92	92	80	94	84	90	100	40	90	90	78	100	88
Scenario 2	52	96	96	64	96	46	96	84	82	70	100	86	88	96	48	98	100	58	92	86
Scenario 3	52	94	84	62	96	46	84	72	72	76	100	74	74	92	42	80	80	70	92	72
Scenario 4	62	96	90	50	100	50	88	82	74	76	98	80	90	90	66	86	86	52	92	80
Average	53.5	95.5	89.5	59.5	97	46	88	82.5	80	75.5	98	81	85.5	94.5	49	88.5	89	64.5	94.5	81.5
Standard deviation (Std)																				
Scenario 1	17.38	4.39	8.67	8.34	1	12.05	10.04	7.62	10.91	2.97	7.37	10.79	12.55	0	13.62	8.92	10.5	3.82	0.44	8
Scenario 2	23.47	18.24	7.08	10.59	5.05	12.3	3.06	17.07	21.28	5.5	0	12.54	28.18	18.27	16.92	0.5	0.16	6.7	5.15	7.29
Scenario 3	19.49	4.51	7.67	5.99	1.78	12.58	8.59	13.19	12.81	7.74	0.13	12.18	12.52	7.74	14.89	8.49	11.4	7.36	5.63	10.95
Scenario 4	12.88	4.39	9.29	9.19	0.37	11.73	8.4	11.37	13.71	5.36	4.34	12.43	9.32	7.41	11.39	9.37	10.89	6.56	4.4	9.61
Average	18.3	7.88	8.18	8.52	2.05	12.17	7.52	12.31	14.68	5.39	2.96	11.98	15.64	8.36	14.21	6.82	8.24	6.11	3.91	8.96
Relative error (RE)																				
Scenario 1	5.81	0.34	1.19	2.26	0.16	3.67	1.61	0.88	1.23	0.82	0.73	1.73	1.6	0	4.39	1.03	1.35	1	0.09	0.88
Scenario 2	9.1	2.26	0.86	3.54	0.57	4.73	0.34	3.67	5.16	1.34	0	2.96	5.88	2.18	5.98	0.09	0.04	2.47	0.64	1.23
Scenario 3	7.36	0.57	1.47	1.72	0.27	4.46	1.65	4.21	4.08	1.8	0.02	3.64	3.78	1.17	6.4	1.68	2.92	1.88	0.71	2.95
Scenario 4	3.35	0.35	1.26	2.73	0.09	3.66	1.04	2.01	3.2	1.16	0.25	2.44	1.22	0.84	2.72	1.36	1.73	2.04	0.4	1.73
Average	6.4	0.88	1.19	2.56	0.27	4.13	1.16	2.7	3.42	1.28	0.25	2.69	3.12	1.05	4.87	1.04	1.51	1.85	0.46	1.7
MAE																				
Scenario 1	14.85	0.88	3.03	5.78	0.4	9.4	4.13	2.26	3.16	2.09	1.87	4.42	4.09	0	11.23	2.64	3.45	2.55	0.23	2.24
Scenario 2	15.58	3.87	1.47	6.06	0.97	8.1	0.58	6.29	8.83	2.29	0	5.06	10.06	3.73	10.23	0.15	0.08	4.22	1.09	2.1
Scenario 3	14.45	1.12	2.88	3.38	0.53	8.76	3.23	8.28	8.01	3.54	0.04	7.16	7.42	2.29	12.58	3.29	5.74	3.7	1.4	5.8
Scenario 4	8.56	0.91	3.21	6.97	0.22	9.37	2.67	5.14	8.17	2.96	0.64	6.24	3.11	2.14	6.96	3.48	4.41	5.21	2.96	4.43
Average	13.36	1.69	2.65	5.55	0.53	8.9	2.65	5.49	7.04	2.72	0.63	5.72	6.17	2.04	10.25	2.39	3.42	3.92	1.42	3.64
RMSE																				
Scenario 1	22.86	4.48	9.19	10.14	1.08	15.28	10.86	7.95	11.36	3.63	7.6	11.66	13.2	0	17.66	9.3	11.06	4.59	0.5	8.3
Scenario 2	28.17	18.65	7.23	12.21	5.14	14.73	3.11	18.19	23.04	5.95	0	13.52	29.92	18.65	19.77	0.53	0.18	7.92	5.26	7.59
Scenario 3	24.25	4.64	8.19	6.87	1.86	15.33	9.17	15.57	15.1	8.51	0.14	14.12	14.55	8.07	19.49	9.1	12.76	8.24	5.8	12.39
Scenario 4	15.46	4.48	9.83	11.53	0.43	15.01	8.81	12.48	15.96	6.13	4.38	13.9	9.82	7.71	13.35	9.99	11.75	8.38	4.52	10.58
Average	22.69	8.06	8.61	10.19	2.13	15.09	7.99	13.55	16.36	6.06	3.03	13.3	16.87	8.61	17.57	7.23	8.94	7.28	4.02	9.72
% Efficiency (Eff.)																				
Scenario 1	94.19	99.66	98.81	97.74	99.84	96.33	98.39	99.12	98.77	99.18	99.27	98.27	98.4	100	95.61	98.97	98.65	99	99.91	99.12
Scenario 2	90.9	97.74	99.14	96.46	99.43	95.27	99.66	96.33	94.84	98.66	100	97.04	94.12	97.82	94.02	99.91	99.96	97.53	99.36	98.77
Scenario 3	92.65	99.43	98.54	98.28	99.73	95.54	98.36	95.79	95.93	98.2	99.99	96.36	96.23	98.84	93.6	98.33	97.08	98.12	99.29	97.05
Scenario 4	96.65	99.65	98.75	97.27	99.91	96.34	98.96	97.99	96.8	98.84	99.75	97.56	98.79	99.16	97.28	98.64	98.27	97.96	99.6	98.27
Average	93.6	99.12	98.81	97.44	99.73	95.87	98.84	97.31	96.58	98.72	99.75	97.31	96.88	98.96	95.13	98.96	98.49	98.15	99.54	98.3

Table A3  
A comparison among considered algorithms and ideal case

Algorithm	Ideal	ALO	DA	DE	FPA	GWO	HS	ICA	MVO	PSO	RMO	Tlbo	WCA	CS	FA	GSA	Jaya	MBA	SCA	WOA	GA
SR	100	53.5	95.5	89.5	59.5	97	46	88	82.5	80	75.5	98	81	85.5	94.5	49	88.5	89	64.5	94.5	81.5
SD	0.0	18.3	7.88	8.18	8.52	2.05	12.17	7.52	12.31	14.68	5.39	2.96	11.98	15.64	8.36	14.21	6.82	8.24	6.11	3.91	8.96
RE	0.0	6.4	0.88	1.19	2.56	0.27	4.13	1.16	2.7	3.42	1.28	0.25	2.69	3.12	1.05	4.87	1.04	1.51	1.85	0.46	1.7
MAE	0.0	13.36	1.69	2.65	5.55	0.53	8.9	2.65	5.49	7.04	2.72	0.63	5.72	6.17	2.04	10.25	2.39	3.42	3.92	1.42	3.64
RMSE	0.0	22.69	8.06	8.61	10.19	2.13	15.09	7.99	13.55	16.36	6.06	3.03	13.3	16.87	8.61	17.57	7.23	8.94	7.28	4.02	9.72
%Eff.	100	93.6	99.12	98.81	97.44	99.73	95.87	98.84	97.31	96.58	98.72	99.75	97.31	96.88	98.96	95.13	98.96	98.49	98.15	99.54	98.3

Table A4  
The detailed performance (obtained maximum power Watt) of each optimizer for the first PSC scenario

Runs	ALO	DA	DE	FPA	GWO	HS	ICA	MVO	PSO	RMO	Tlbo	WCA	CS	FA	GSA	Jaya	MBA	SCA	WOA	GA
1	255.7	255.69	255.7	253.99	255.01	250.73	224.45	255.7	255.7	254.06	255.7	255.7	255.7	255.7	255.68	250.95	255.69	255.57	255.64	254.58
2	255.7	255.68	255.7	232.46	255.68	216.15	255.69	255.69	255.69	255.57	255.7	255.69	255.7	255.7	232.1	255.7	255.69	255.66	255.65	255.69
3	228.99	255.21	255.7	236.23	255.7	255.7	255.7	255.67	255.7	254.87	255.7	255.7	255.7	255.7	219.58	224.57	224.66	255.7	255.68	255.39
4	218.2	255.18	255.66	255.7	255.68	251.93	255.7	255.66	255.7	247.19	255.7	255.7	255.7	255.7	224.05	255.66	255.69	255.68	255.64	255.69
5	220.27	255.56	255.7	255.22	255.65	245.85	255.7	255.7	255.7	254.42	255.7	255.7	255.7	255.7	223.86	255.59	255.68	255.69	255.68	255.57
6	224.53	255.69	255.7	238.44	255.67	228.41	255.7	255.44	255.69	253.37	255.7	255.7	255.7	255.7	237.34	253.39	255.7	254.49	255.7	255.65
7	255.7	255.7	255.7	253.93	255.53	255.35	253.27	255.6	255.7	255.12	255.7	224.66	255.7	255.7	255.66	255.61	255.69	255.7	255.69	255.69
8	255.7	255.7	255.7	255.41	253.8	255.01	255.13	255.65	255.61	248.93	255.69	224.66	255.7	255.7	252.14	255.7	255.6	255.66	255.6	255.55
9	224.66	255.69	255.7	254.08	255.69	242.09	255.7	255.63	208.13	255.69	255.7	224.66	255.7	255.7	253.49	255.49	255.7	255.53	255.64	255.69
10	255.69	255.65	255.69	253.36	255.66	248.16	255.7	255.67	255.7	255.7	255.7	255.7	255.7	255.7	247.31	255.29	255.69	255.68	255.23	255.69
11	224.66	255.64	255.7	241.58	252.3	242.27	255.69	255.68	255.68	255.59	255.7	255.7	255.7	255.7	251.13	255.7	255.68	255.7	255.57	255.69
12	255.7	255.7	255.7	255.62	255.55	255.63	255.7	255.69	255.55	254.34	255.7	255.7	255.7	255.7	255.65	255.6	255.7	255.39	255.69	255.66
13	253.56	224.66	255.69	254.35	255.34	241.26	255.7	224.66	255.68	253.24	255.7	255.7	255.7	255.7	240.17	255.69	255.7	255.61	254.88	255.32
14	210.57	255.66	255.69	252.47	255.69	255.69	255.7	255.69	208.14	253.03	255.7	255.7	255.7	255.7	253.99	255.7	255.7	255.69	255.7	254.84
15	255.7	255.64	224.58	255.64	255.7	252.84	255.69	255.69	255.7	253.41	255.7	255.7	255.7	255.7	255.68	255.69	255.65	255.68	255.7	255.51
16	231.2	255.65	255.7	247.2	255.01	243.4	255.65	255.3	255.69	255.53	255.7	255.7	255.7	255.7	240.1	255.53	255.7	255.56	255.69	255.39
17	255.7	255.68	224.65	226.63	255.7	215.86	255.37	255.56	255.7	255.13	224.66	224.66	255.7	255.7	255.7	255.62	255.69	255.7	255.67	253.54
18	248.34	255.64	255.59	253.23	255.69	248.93	255.7	255.69	255.7	255.7	255.7	255.7	255.7	255.7	224.65	224.66	255.69	255.69	255.69	254.82
19	246.38	255.13	242.28	250.96	255.68	255.67	255.67	255.21	255.7	255.59	255.68	224.66	208.16	208.16	253.94	255.55	255.69	255.67	255.05	255.69
20	255.69	249.77	255.7	251.73	255.44	254.74	224.66	255.68	224.66	255.58	255.7	255.7	208.16	208.16	225.89	255.69	255.57	255.58	255.7	255.61
21	255.7	255.62	255.7	252.62	255.62	248.79	255.69	255.63	255.67	244.19	255.7	255.7	255.7	255.7	255.7	255.63	254.76	255.38	255.51	255.69
22	224.66	255.42	255.67	253.68	255.6	225.85	255.67	255.67	255.7	255.64	255.7	255.7	255.7	255.7	255.7	255.7	255.7	255.69	255.7	255.69
23	255.7	255.66	255.7	254.59	255.47	245.24	255.68	255.69	255.7	252.3	255.7	255.7	255.7	255.7	208.08	254.45	255.7	255.66	255.69	255.69

(continued on next page)

Table A4 (continued)

Runs	ALO	DA	DE	FPA	GWO	HS	ICA	MVO	PSO	RMO	Tlbo	WCA	CS	FA	GSA	Jaya	MBA	SCA	WOA	GA
24	255.7	255.7	255.7	255.67	254.21	254.53	255.7	255.58	255.69	253.4	255.7	255.7	255.7	255.69	224.91	245.53	255.69	255.69	255.65	255.61
25	224.66	255.67	255.64	255.65	254.17	240.43	255	255.67	255.69	255.22	255.7	252.78	255.7	255.7	240.99	255.61	255.66	224.66	255.7	255.69
26	255.59	255.7	255.67	255.68	255.6	255.68	255.7	255.68	255.7	245.92	255.7	255.7	255.7	255.7	254.85	255.69	255.7	255.59	255.5	255.69
27	255.7	255.05	255.7	248.34	255.65	253.54	255.7	255.52	255.7	246.83	255.7	255.7	208.13	255.7	242.22	255.7	255.7	255.66	255.68	255.57
28	255.7	255.67	224.66	255.1	255.64	224.63	255.7	255.54	255.7	255.25	255.7	255.7	255.7	255.7	251.92	255.7	255.7	254.18	255.69	248.61
29	224.66	255.69	255.7	255.21	255.7	255.37	253.34	255.69	255.69	255.68	224.66	255.7	255.7	255.7	240.3	255.68	255.69	255.66	255.61	252.76
30	250.32	255.7	255.69	240.85	255.25	253.74	249.2	255.12	255.7	253.68	255.7	255.7	255.7	255.7	245.95	255.69	255.7	255.7	255.53	208.16
31	255.7	254.79	255.69	255.32	255.69	242.7	255.7	255.55	255.69	255.68	255.7	255.7	255.7	255.7	248.06	255.69	224.66	255.67	255.52	255.69
32	244.38	255.69	255.7	252.59	255.56	255.36	255.69	224.59	255.68	250.9	255.69	224.66	224.66	255.7	253.62	255.7	255.7	255.68	254.53	255.69
33	245.01	255.49	255.7	253.38	255.62	253.13	249	255.69	255.7	254.23	255.7	255.7	255.7	255.7	251.01	255.7	255.7	255.65	255.7	255.55
34	223.81	255.69	255.67	254.07	255.69	250.55	255.7	255.61	255.7	254.48	255.7	255.7	255.7	255.7	253.87	255.21	255.52	255.68	255.68	252.61
35	224.66	254.17	255.7	255.48	255.64	255.7	255.69	255.68	255.7	254.17	255.7	255.7	255.7	255.7	236.06	255.68	255.7	255.7	255.33	255.69
36	255.7	255.67	255.7	252.32	249.65	255.69	255.7	255.69	255.7	245.09	255.7	223.96	255.7	255.7	243.81	255.7	255.69	255.67	255.22	255.69
37	241.7	255.7	255.7	239.05	255.66	240.7	224.65	255.67	224.66	255.7	255.7	255.7	255.7	255.7	255.05	255.7	255.65	255.66	254.43	255.69
38	235.07	255.68	255.57	224.65	255.28	204.21	255.64	255.65	255.68	255.69	255.7	255.7	255.7	255.7	248.84	255.7	255.7	255.54	255.68	255.15
39	255.69	255.65	255.7	254.82	255.64	255.59	255.69	255.69	255.68	255.45	255.7	255.58	255.7	255.7	218.98	255.7	255.5	255.57	255.68	255.67
40	208.36	255.69	255.7	254.95	255.69	247.61	255.69	255.68	255.68	255.58	255.7	255.7	255.7	255.7	255.69	255.69	255.7	255.68	254.86	255.69
41	221.88	255.68	242.32	255.67	255.69	240.79	224.66	255.69	255.69	251.49	224.66	255.7	224.66	255.7	255.69	255.58	224.66	255.65	255.69	255.63
42	255.7	255.69	255.7	229.23	255.68	255.04	255.65	255.69	255.7	254.96	255.7	255.7	255.7	255.7	249.85	255.48	255.69	255.65	255.68	255.68
43	255.7	255.47	224.66	235.64	255.43	253.26	224.66	224.62	255.56	255.64	255.52	255.7	255.7	255.7	246.79	255.69	255.69	255.59	255.7	255.69
44	224.66	255.69	255.67	248.23	255.68	250.87	255.7	255.58	255.7	254.56	255.7	255.69	255.7	255.7	252.81	255.61	255.7	255.67	255.69	255.69
45	255.63	255.7	255.69	253.1	255.49	249.81	255.7	255.7	255.69	254.53	255.7	255.7	255.7	255.7	255.48	255.7	224.66	255.69	255.66	255.65
46	201.11	255.56	255.69	254.57	255.61	224.51	255.7	255.7	255.7	255.52	255.7	255.7	255.7	255.7	255.53	255.69	255.69	255.38	255.69	243.56
47	255.7	255.61	255.7	253.77	255.44	255.68	255.7	255.69	255.7	255.57	255.7	255.7	255.7	255.7	255.5	255.7	255.68	255.69	255.37	255.69
48	241.09	255.55	255.7	254.53	255.62	249.41	255.68	239.6	255.67	254.34	255.7	255.7	255.7	255.7	249.54	255.7	255.7	255.65	255.69	255.33
49	255.7	255.52	255.7	253.82	255.58	255.6	224.66	255.68	255.7	255.16	255.69	255.7	255.7	255.7	202.91	255.45	208.16	255.39	254.69	255.67
50	194.39	255.7	255.7	255.41	255.63	245.55	255.7	255.69	255.7	251.51	255.7	255.7	255.7	255.7	255.64	208.16	255.68	255.67	255.27	224.66

## References

- [1] Kabir E, Kumar P, Kumar S, Adelodun AA, Kim K-H. Solar energy: potential and future prospects. *Renew Sustain Energy Rev* 2018;82:894–900.
- [2] Danandeh M. Comparative and comprehensive review of maximum power point tracking methods for PV cells. *Renew Sustain Energy Rev* 2018;82:2743–67.
- [3] Kermadi M, Berkouk EM. Artificial intelligence-based maximum power point tracking controllers for photovoltaic systems: comparative study. *Renew Sustain Energy Rev* 2017;69:369–86.
- [4] Ali AI, Sayed MA, Mohamed EE. Modified efficient perturb and observe maximum power point tracking technique for grid-tied PV system. *Int J Electr Power Energy Syst* 2018;99:192–202.
- [5] Al-Najideen MI, Alrwashdeh SS. Design of a solar photovoltaic system to cover the electricity demand for the faculty of Engineering-Mu'tah University in Jordan. *Resour-Efficient Technol* 2017;3:440–5.
- [6] Marmoush MM, Rezk H, Shehata N, Henry J, Gomaa MR. A novel merging tubular daylight device with solar water heater—experimental study. *Renew Energy* 2018;125:947–61.
- [7] Hemeida M, Rezk H, Hamada MM. A comprehensive comparison of STATCOM versus SVC-based fuzzy controller for stability improvement of wind farm connected to multi-machine power system. *Electr Eng* 2017;1–17.
- [8] Atems B, Hotaling C. The effect of renewable and nonrenewable electricity generation on economic growth. *Energy Policy* 2018;112:111–8.
- [9] Çelik Ö, Teke A, Tan A. Overview of micro-inverters as a challenging technology in photovoltaic applications. *Renew Sustain Energy Rev* 2018;82:3191–206.
- [10] Azzouzi M, Popescu D, Bouchahdane M. Modeling of electrical characteristics of photovoltaic cell considering single-diode model. *J Clean Energy Technol* 2016;4:414–20.
- [11] Shahid H, Kamran M, Mehmood Z, Saleem MY, Mudassar M, Haider K. Implementation of the novel temperature controller and incremental conductance MPPT algorithm for indoor photovoltaic system. *Sol Energy* 2018;163:235–42.
- [12] Sarkar MNI. Effect of various model parameters on solar photovoltaic cell simulation: a SPICE analysis. *Renew: Wind, Water, and Solar* 2016;3:13.
- [13] Kamran M, Mudassar M, Fazal MR, Asghar MU, Bilal M, Asghar R. Implementation of improved Perturb & Observe MPPT technique with confined search space for standalone photovoltaic system. *Journal of King Saud University-Engineering Sciences*; 2018.
- [14] Rezk H, Tyukhov I, Raupov A. Experimental implementation of meteorological data and photovoltaic solar radiation monitoring system. *Int Transac Elec Energy Syst* 2015;25:3573–85.
- [15] Rezk H, Tyukhov I, Al-Dhaifallah M, Tikhonov A. Performance of data acquisition system for monitoring PV system parameters. *Measurement* 2017;104:204–11.
- [16] Bahrami M, Gavagsaz-Ghoachani R, Zandi M, Phattanasak M, Maranzana G, Nahid-Mobarakeh B, et al. Hybrid maximum power point tracking algorithm with improved dynamic performance. *Renew Energy* 2019;130:982–91.
- [17] Soufi Y, Bechouat M, Kahla S. Fuzzy-PSO controller design for maximum power point tracking in photovoltaic system. *Int J Hydrogen Energy* 2017;42:8680–8.
- [18] Rezk H, El-Sayed AHM. Sizing of a stand alone concentrated photovoltaic system in Egyptian site. *Int J Electr Power Energy Syst* 2013;45:325–30.
- [19] Díaz-Dorado E, Cidrás J, Carrillo C. A method to estimate the energy production of photovoltaic trackers under shading conditions. *Energy Convers Manag* 2017;150:433–50.
- [20] Rezk H. A comprehensive sizing methodology for stand-alone battery-less photovoltaic water pumping system under the Egyptian climate. *Cogent Eng* 2016;3:1242110.
- [21] Rezk H, Dousoky GM. Technical and economic analysis of different configurations of stand-alone hybrid renewable power systems—A case study. *Renew Sustain Energy Rev* 2016;62:941–53.
- [22] Peng L, Zheng S, Chai X, Li L. A novel tangent error maximum power point tracking algorithm for photovoltaic system under fast multi-changing solar irradiances. *Appl Energy* 2018;210:303–16.
- [23] Armghan H, Ahmad I, Armghan A, Khan S, Arsalan M. Backstepping based nonlinear control for maximum power point tracking in photovoltaic system. *Sol Energy* 2018;159:134–41.
- [24] Bouselham L, Hajji M, Hajji B, Bouali H. A new MPPT-based ANN for photovoltaic system under partial shading conditions. *Energy Procedia* 2017;111:924–33.
- [25] Balato M, Vitelli M. Optimization of distributed maximum power point tracking PV applications: the scan of the Power vs. Voltage input characteristic of the inverter. *Int J Electr Power Energy Syst* 2014;60:334–46.
- [26] Titri S, Larbes C, Toumi KY, Benatchba K. A new MPPT controller based on the Ant colony optimization algorithm for Photovoltaic systems under partial shading conditions. *Appl Soft Comput* 2017;58:465–79.
- [27] Al-Majidi SD, Abbod MF, Al-Rawashidi HS. A novel maximum power point tracking technique based on fuzzy logic for photovoltaic systems. *Int J Hydrogen Energy* 2018;43:14158–71.
- [28] Karami N, Moubayed N, Outbib R. General review and classification of different MPPT Techniques. *Renew Sustain Energy Rev* 2017;68:1–18.
- [29] Motahhir S, El Hammoumi A, El Ghzizal A. Photovoltaic system with quantitative comparative between an improved MPPT and existing INC and P&O methods under fast varying of solar irradiation. *Energy Rep* 2018;4:341–50.
- [30] Li X, Wen H, Hu Y, Jiang L. A novel beta parameter based fuzzy-logic controller for photovoltaic MPPT application. *Renew Energy* 2019;130:416–27.
- [31] Ponkarthik N, Murugavel KK. Performance enhancement of solar photovoltaic system using novel Maximum Power Point Tracking. *Int J Electr Power Energy Syst* 2014;60:1–5.
- [32] Messalti S, Harrag A, Loukriz A. A new variable step size neural networks MPPT controller: review, simulation and hardware implementation. *Renew Sustain Energy Rev* 2017;68:221–33.
- [33] Sampaio PGV, González MOA. Photovoltaic solar energy: conceptual framework. *Renew Sustain Energy Rev* 2017;74:590–601.
- [34] Tolba M, Rezk H, Diab A, Al-Dhaifallah M. A novel robust methodology based Salp swarm algorithm for allocation and capacity of renewable distributed generators on distribution grids. *Energies* 2018;11:2556.
- [35] Moshksar E, Ghanbari T. A model-based algorithm for maximum power point tracking of PV systems using exact analytical solution of single-diode equivalent model. *Sol Energy* 2018;162:117–31.
- [36] Camilo JC, Guedes T, Fernandes DA, Melo J, Costa F, Sguarezi Filho AJ. A maximum power point tracking for photovoltaic systems based on Monod equation. *Renew Energy* 2019;130:428–38.
- [37] Al-omary M, Kaltschmitt M, Becker C. Electricity system in Jordan: status & prospects. *Renewable and Sustainable Energy Reviews*; 2017.
- [38] Motahhir S, Chalh A, El Ghzizal A, Derouich A. Development of a low-cost PV system using an improved INC algorithm and a PV panel Proteus model. *J Clean Prod* 2018;204:355–65.
- [39] Bana S, Saini R. Experimental investigation on power output of different photovoltaic array configurations under uniform and partial shading scenarios. *Energy* 2017;127:438–53.
- [40] Al Mamun MA, Hasanuzzaman M, Selvaraj J. Experimental investigation of the effect of partial shading on photovoltaic performance. *IET Renew Power Gener* 2017;11:912–21.
- [41] Dhimish M, Holmes V, Mehrdadi B, Dales M, Chong B, Zhang L. Seven indicators variations for multiple PV array configurations under partial shading and faulty PV conditions. *Renew Energy* 2017;113:438–60.
- [42] Yadav AS, Pachauri RK, Chauhan YK, Choudhury S, Singh R. Performance enhancement of partially shaded PV array using novel shade dispersion effect on magic-square puzzle configuration. *Sol Energy* 2017;144:780–97.
- [43] Bayrak F, Ertürk G, Oztok HF. Effects of partial shading on energy and exergy efficiencies for photovoltaic panels. *J Clean Prod* 2017;164:58–69.
- [44] Eltamaly AM, Farh HM, Othman MF. A novel evaluation index for the photovoltaic maximum power point tracker techniques. *Sol Energy* 2018;174:940–56.
- [45] Belhachat F, Larbes C. Global maximum power point tracking based on ANFIS approach for PV array configurations under partial shading conditions. *Renew Sustain Energy Rev* 2017;77:875–89.
- [46] Alik R, Jusoh A. An enhanced P&O checking algorithm MPPT for high tracking efficiency of partially shaded PV module. *Sol Energy* 2018;163:570–80.
- [47] Ishaque K, Salam Z. A review of maximum power point tracking techniques of PV system for uniform insolation and partial shading condition. *Renew Sustain Energy Rev* 2013;19:475–88.
- [48] Rezk H, Hasanene E-S. A new MATLAB/Simulink model of triple-junction solar cell and MPPT based on artificial neural networks for photovoltaic energy systems. *Ain Shams Eng J* 2015;6:873–81.
- [49] Issaadi Y, Issaadi S, Khireddine A. Comparative study of photovoltaic system optimization techniques: contribution to the improvement and development of new approaches. *Renew Sustain Energy Rev* 2018;82:2112–27.
- [50] Rezk H, Eltamaly AM. A comprehensive comparison of different MPPT techniques for photovoltaic systems. *Sol Energy* 2015;112:1–11.
- [51] Aldair AA, Obed AA, Halihal AF. Design and implementation of ANFIS-reference model controller based MPPT using FPGA for photovoltaic system. *Renew Sustain Energy Rev* 2018;82:2202–17.
- [52] Seyedmahmoudian M, Horan B, Soon TK, Rahmani R, Oo AMT, Mekhilef S, et al. State of the art artificial intelligence-based MPPT techniques for mitigating partial shading effects on PV systems—A review. *Renew Sustain Energy Rev* 2016;64:435–55.
- [53] Avila E, Pozo N, Pozo M, Salazar G, Domínguez X. Improved particle swarm optimization based MPPT for PV systems under Partial Shading Conditions. *Power electronics conference (SPEC), 2017 IEEE southern: IEEE*. 2017. p. 1–6.
- [54] Gavhane PS, Krishnamurthy S, Dixit R, Ram JP, Rajasekar N. EL-PSO based MPPT for solar PV under partial shaded condition. *Energy Procedia* 2017;117:1047–53.
- [55] Liu Y-H, Huang S-C, Huang J-W, Liang W-C. A particle swarm optimization-based maximum power point tracking algorithm for PV systems operating under partially shaded conditions. *IEEE Trans Energy Convers* 2012;27:1027–35.
- [56] Dwivedi M, Mehta G, Iqbal A, Shekhar H. Performance enhancement of solar PV system under partial shaded condition using PSO. 2017 8th international conference on computing, communication and networking technologies (ICCCNT). IEEE; 2017. p. 1–7.
- [57] Eltamaly AM, Farh H MH, Al Saud M S. Impact of PSO reinitialization on the accuracy of dynamic global maximum power detection of variant partially shaded PV systems. *Sustainability* 2019;11:2091.
- [58] Farh HMH, Othman MF, Eltamaly AM, Al-Saud MS. Maximum power extraction from a partially shaded PV system using an interleaved boost converter. *Energies* 2018;11:2543.
- [59] Dileep G, Singh SN. An improved particle swarm optimization based maximum power point tracking algorithm for PV system operating under partial shading conditions. *Sol Energy* 2017;158:1006–15.
- [60] Rezk H, Fathy A, Abdelaziz AY. A comparison of different global MPPT techniques based on meta-heuristic algorithms for photovoltaic system subjected to partial shading conditions. *Renew Sustain Energy Rev* 2017;74:377–86.
- [61] Taheri H, Salam Z, Ishaque K. A novel maximum power point tracking control of photovoltaic system under partial and rapidly fluctuating shadow conditions using differential evolution. *Industrial electronics & applications (ISIEA), 2010 IEEE symposium on: IEEE*. 2010. p. 82–7.

- [62] Tey KS, Mekhilef S, Seyedmehmoudian M, Horan B, Oo AMT, Stojcevski A. Improved differential evolution-based MPPT algorithm using SEPIC for PV systems under partial shading conditions and load variation. *IEEE Transac Indus Inform* 2018.
- [63] Kumar N, Hussain I, Singh B, Panigrahi BK. MPPT in dynamic condition of partially shaded PV system by using WODE technique. *IEEE Transac Sustain Energy* 2017;8:1204–14.
- [64] Kumar N, Hussain I, Singh B, Panigrahi BK. Rapid MPPT for uniformly and partial shaded PV system by using JayaDE algorithm in highly fluctuating atmospheric conditions. *IEEE Transac Indus Inform* 2017;13:2406–16.
- [65] Ram JP, Rajasekar N. A new global maximum power point tracking technique for solar photovoltaic (PV) system under partial shading conditions (PSC). *Energy* 2017;118:512–25.
- [66] Subha R, Himavathi S. MPPT of PV systems under partial shaded conditions using flower pollination algorithm. 2017 international conference on innovations in electrical, electronics, instrumentation and media technology (ICEEIMT). 2017. p. 206–10.
- [67] Diab AAZ, Rezk H. Global MPPT based on flower pollination and differential evolution algorithms to mitigate partial shading in building integrated PV system. *Sol Energy* 2017;157:171–86.
- [68] Chao K-H, Wu M-C. Global maximum power point tracking (MPPT) of a photovoltaic module array constructed through improved teaching-learning-based optimization. *Energies* 2016;9:986.
- [69] Fathy A, Ziedan I, Amer D. Improved teaching-learning-based optimization algorithm-based maximum power point trackers for photovoltaic system. *Electr Eng* 2017;1–12.
- [70] Patsariya A, Rai S, Kumar Y, Kiran M. Noble-tlbo MPPT technique and its comparative analysis with conventional methods implemented on solar photovoltaic system. IOP conference series: materials science and engineering: IOP publishing. 2017. p. 012048.
- [71] Mohanty S, Subudhi B, Ray PK. A new MPPT design using grey wolf optimization technique for photovoltaic system under partial shading conditions. *IEEE Transac Sustain Energy* 2016;7:181–8.
- [72] Mohanty S, Subudhi B, Ray PK. A grey wolf-assisted perturb & observe MPPT algorithm for a PV system. *IEEE Trans Energy Convers* 2017;32:340–7.
- [73] Sarvi M, Soltani I, Avnaki I. A water cycle algorithm maximum power point tracker for photovoltaic energy conversion system under partial shading condition. *Appl Math Eng Manag Technol* 2014;2:103–16.
- [74] Fathy A, Rezk H. A novel methodology for simulating maximum power point trackers using mine blast optimization and teaching learning based optimization algorithms for partially shaded photovoltaic system. *J Renew Sustain Energy* 2016;8:023503.
- [75] Sahu RK, Shaw B. Design of solar system by implementing ALO optimized PID based MPPT controller. *Trends Renew Energy* 2018;4:44–55.
- [76] Kumar N, Hussain I, Singh B, Panigrahi BK. Maximum power extraction from partially shaded PV panel in rainy season by using improved antlions optimization algorithm. 2016 IEEE 7th power India international conference (PIICON). 2016. p. 1–6.
- [77] Vedadi M, Vahidi B, Hosseini SH. An imperialist competitive algorithm maximum power point tracker for photovoltaic string operating under partially shaded conditions. *Sci Int* 2015;27:4023–33.
- [78] Seyedmehmoudian M, Horan B, Rahmani R, Maung Than Oo A, Stojcevski A. Efficient photovoltaic system maximum power point tracking using a new technique. *Energies* 2016;9:147.
- [79] Kumar CS, Rao RS. A novel global MPP tracking of photovoltaic system based on whale optimization algorithm. *Int J Renew Energy Dev* 2016;5:225–32.
- [80] Kumar N, Hussain I, Singh B, Panigrahi BK. Single sensor-based MPPT of partially shaded PV system for battery charging by using Cauchy and Gaussian sine cosine optimization. *IEEE Trans Energy Convers* 2017;32:983–92.
- [81] Saha D. A GSA based improved MPPT algorithm for PV generation. Research in computational intelligence and communication networks (ICRCICN), 2015 IEEE international conference on. IEEE; 2015. p. 131–6.
- [82] Zheng Y, Wei C, Lin S. A maximum power point tracking method based on tabu search for PV systems under partially shaded conditions. 2011.
- [83] Sridhar R, Jeevananthan S, Dash SS, Vishnuram P. A new maximum power tracking in PV system during partially shaded conditions based on shuffled frog leap algorithm. *J Exp Theor Artif Intell* 2017;29:481–93.
- [84] Ahmed J, Salam Z. A maximum power point tracking (MPPT) for PV system using cuckoo search with partial shading capability. *Appl Energy* 2014;119:118–30.
- [85] Sundareswaran K, Peddapati S, Palani S. MPPT of PV systems under partial shaded conditions through a colony of flashing fireflies. *IEEE Trans Energy Convers* 2014;29:463–72.
- [86] Teshome D, Lee C, Lin Y, Lian K. A modified firefly algorithm for photovoltaic maximum power point tracking control under partial shading. *IEEE J Emerg Select Topics Power Electron* 2017;5:661–71.
- [87] Hadji S, Gaubert J-P, Krim F. Genetic algorithms for maximum power point tracking in photovoltaic systems. *Power Electronics and Applications (EPE 2011). Proceedings of the 2011-14th European conference on: IEEE.* 2011. p. 1–9.
- [88] Ramaprabha R, Gothandaraman V, Kanimozhi K, Divya R, Mathur B. Maximum power point tracking using GA-optimized artificial neural network for Solar PV system. *Electrical energy systems (ICEES), 2011 1st international conference on: IEEE.* 2011. p. 264–8.
- [89] Bakhshi R, Sadeh J, Mosaddegh H-R. Optimal economic designing of grid-connected photovoltaic systems with multiple inverters using linear and nonlinear module models based on Genetic Algorithm. *Renew Energy* 2014;72:386–94.
- [90] Huang C, Wang L, Yeung RS-C, Zhang Z, Chung HS-H, Bensoussan A. A prediction model-guided Jaya algorithm for the PV system maximum power point tracking. *IEEE Transac Sustain Energy* 2018;9:45–55.
- [91] Belhaouas N, Cheikh M-SA, Agathoklis P, Oularbi M-R, Amrouche B, Sedraoui K, et al. PV array power output maximization under partial shading using new shifted PV array arrangements. *Appl Energy* 2017;187:326–37.
- [92] Kandemir E, Cetin NS, Borekci S. A comprehensive overview of maximum power extraction techniques for PV systems. *Renew Sustain Energy Rev* 2017;78:93–112.
- [93] Li G, Jin Y, Akram M, Chen X, Ji J. Application of bio-inspired algorithms in maximum power point tracking for PV systems under partial shading conditions—A review. *Renew Sustain Energy Rev* 2018;81:840–73.
- [94] Ahmad R, Murtaza AF, Sher HA, Shami UT, Olalekan S. An analytical approach to study partial shading effects on PV array supported by literature. *Renew Sustain Energy Rev* 2017;74:721–32.
- [95] Malathy S, Ramaprabha R. Reconfiguration strategies to extract maximum power from photovoltaic array under partially shaded conditions. *Renew Sustain Energy Rev* 2018;81:2922–34.
- [96] Balato M, Vitelli M. A new control strategy for the optimization of distributed MPPT in PV applications. *Int J Electr Power Energy Syst* 2014;62:763–73.
- [97] Kumar Dash S, Nema S, Nema R, Verma D. A comprehensive assessment of maximum power point tracking techniques under uniform and non-uniform irradiance and its impact on photovoltaic systems: a review. *J Renew Sustain Energy* 2015;7:063113.
- [98] Tolba M, Rezk H, Tulsy V, Diab A, Abdelaziz A, Vanin A. Impact of optimum allocation of renewable distributed generations on distribution networks based on different optimization algorithms. *Energies* 2018;11:245.
- [99] Sarvi M, Ahmadi S, Abdi S. A PSO-based maximum power point tracking for photovoltaic systems under environmental and partially shaded conditions. *Prog Photovolt Res Appl* 2015;23:201–14.
- [100] Danandeh MA, Mousavi GSM. Comparative and comprehensive review of maximum power point tracking methods for PV cells. *Renew Sustain Energy Rev* 2018;82:2743–67.
- [101] Jouda A, Elyes F, Rabhi A, Abdelkader M. Optimization of scaling factors of fuzzy-MPPT controller for stand-alone photovoltaic system by particle swarm optimization. *Energy Procedia* 2017;111:954–63.
- [102] Jiang LL, Srivatsan R, Maskell DL. Computational intelligence techniques for maximum power point tracking in PV systems: a review. *Renew Sustain Energy Rev* 2018;85:14–45.
- [103] Ramli MAM, Twaha S, Ishaque K, Al-Turki YA. A review on maximum power point tracking for photovoltaic systems with and without shading conditions. *Renew Sustain Energy Rev* 2017;67:144–59.
- [104] Ram JP, Babu TS, Rajasekar N. A comprehensive review on solar PV maximum power point tracking techniques. *Renew Sustain Energy Rev* 2017;67:826–47.
- [105] Batarseh MG, Zafer ME. Hybrid maximum power point tracking techniques: a comparative survey, suggested classification and uninvestigated combinations. *Sol Energy* 2018;169:535–55.
- [106] Chaieb H, Sakly A. A novel MPPT method for photovoltaic application under partial shaded conditions. *Sol Energy* 2018;159:291–9.
- [107] Tajuddin M, Arif M, Ayob S, Salam Z. Perturbative methods for maximum power point tracking (MPPT) of photovoltaic (PV) systems: a review. *Int J Energy Res* 2015;39:1153–78.
- [108] Tajuddin MFN, Arif MS, Ayob SM, Salam Z. Perturbative methods for maximum power point tracking (MPPT) of photovoltaic (PV) systems: a review. *Int J Energy Res* 2015;39:1153–78.
- [109] Yang X-S, Karamanoglu M, He X. Flower pollination algorithm: a novel approach for multiobjective optimization. *Eng Optim* 2014;46:1222–37.
- [110] Kler D, Rana KPS, Kumar V. A nonlinear PID controller based novel maximum power point tracker for PV systems. *J Frankl Inst* 2018;355:7827–64.
- [111] Rao RV, Savsani VJ, Vakharia D. Teaching-learning-based optimization: an optimization method for continuous non-linear large scale problems. *Inf Sci* 2012;183:1–15.
- [112] Rezk H, Fathy A. Simulation of global MPPT based on teaching-learning-based optimization technique for partially shaded PV system. *Electr Eng* 2017;99:847–59.
- [113] Rezk H, Fathy A. A novel optimal parameters identification of triple-junction solar cell based on a recently meta-heuristic water cycle algorithm. *Sol Energy* 2017;157:778–91.
- [114] Li Q, Chen H, Huang H, Zhao X, Cai Z, Tong C, et al. An enhanced grey wolf optimization based feature selection wrapped kernel extreme learning machine for medical diagnosis. *Comput Mathematical Methods Med* 2017;2017.
- [115] Rajkumar DV, Mahakumar M, Manojkumar M, Hemaraj M, Kumaravel E. A new DC-DC converter topology with grey wolf MPPT algorithm for photovoltaic system. *Int J Emerg Trends Eng Res* 2017;5:54–9.
- [116] Cherukuri SK, Rayapudi SR. Enhanced grey wolf optimizer based MPPT algorithm of PV system under partial shaded condition. *Int J Renew Energy Dev* 2017;6:203.
- [117] Mohapatra A, Nayak B, Das P, Mohanty KB. A review on MPPT techniques of PV system under partial shading condition. *Renew Sustain Energy Rev* 2017;80:854–67.
- [118] Diab AAZ, Rezk H. Optimal sizing and placement of capacitors in radial distribution systems based on grey wolf, dragonfly and moth-flame optimization algorithms. *Iranian J Sci Technol Transac Electr Eng*. 1-20.
- [119] Mohamed MA, Zaki Diab AA, Rezk H. Partial shading mitigation of PV systems via different meta-heuristic techniques. *Renew Energy* 2019;130:1159–75.
- [120] Eskandar H, Sadollah A, Bahreininejad A, Hamdi M. Water cycle algorithm—A novel metaheuristic optimization method for solving constrained engineering optimization problems. *Comput Struct* 2012;110:151–66.
- [121] Ghaffarzadeh N. Water cycle algorithm based power system stabilizer robust

- design for power systems. *J Electr Eng* 2015;66:91–6.
- [122] Kumar N, Hussain I, Singh B, Panigrahi BK. Normal harmonic search algorithm-based MPPT for solar PV system and integrated with grid using reduced sensor approach and PNKLS algorithm. *IEEE Trans Ind Appl* 2018;54:6343–52.
- [123] Kim JH. Harmony search algorithm: a unique music-inspired algorithm. *Procedia Eng* 2016;154:1401–5.
- [124] Mirjalili S. Dragonfly algorithm: a new meta-heuristic optimization technique for solving single-objective, discrete, and multi-objective problems. *Neural Comput Appl* 2016;27:1053–73.
- [125] Venkatesh M, Sudheer G. Optimal load frequency regulation OF micro-grid using dragonfly algorithm. 2017.
- [126] Bashishtha TK, Srivastava L. Nature inspired meta-heuristic dragonfly algorithms for solving optimal power flow problem. *Nature* 2016.
- [127] KS SR, Murugan S. Memory based hybrid dragonfly algorithm for numerical optimization problems. *Expert Syst Appl* 2017;83:63–78.
- [128] Zawbaa HM, Emary E, Parv B. Feature selection based on antlion optimization algorithm. *Complex Systems (WCCS)*, 2015 Third World Conference on. *IEEE*; 2015. p. 1–7.
- [129] Dubey R, Joshi D, Bansal RC. Optimization of solar photovoltaic plant and economic analysis. *Electr Power Compon Syst* 2016;44:2025–35.
- [130] Abdollahi M, Isazadeh A, Abdollahi D. Imperialist competitive algorithm for solving systems of nonlinear equations. *Comput Math Appl* 2013;65:1894–908.
- [131] Fathy A, Rezk H. Parameter estimation of photovoltaic system using imperialist competitive algorithm. *Renew Energy* 2017;111:307–20.
- [132] Vanithasri M, Balamurugan R, Lakshminarasimman L. Radial movement optimization (RMO) technique for solving unit commitment problem in power systems. *J Elect Syst Inform Technol* 2017.
- [133] Al-Dhaifallah M, Nassef AM, Rezk H, Nisar KS. Optimal parameter design of fractional order control based INC-MPPT for PV system. *Sol Energy* 2018;159:650–64.
- [134] Vanithasri M, Balamurugan R, Lakshminarasimman L. Modified radial movement optimization (MRMO) technique for estimating the parameters of fuel cost function in thermal power plants. *Eng Sci Technol Int J* 2016;19:2035–42.
- [135] Fathy A, Rezk H. Multi-verse optimizer for identifying the optimal parameters of PEMFC model. *Energy* 2018;143:634–44.
- [136] Mirjalili S, Mirjalili SM, Hatamlou A. Multi-verse optimizer: a nature-inspired algorithm for global optimization. *Neural Comput Appl* 2016;27:495–513.
- [137] Jangir P, Parmar SA, Trivedi IN, Bhesdadiya R. A novel hybrid particle swarm optimizer with multi verse optimizer for global numerical optimization and optimal reactive power dispatch problem. *Eng Sci Technol Int J* 2017;20:570–86.
- [138] Sulaiman MH, Mohamed MR, Mustafa Z, Aliman O. An application of multi-verse optimizer for optimal reactive power dispatch problems. *Int J Simul Syst Sci Technol* 2016;17:41.
- [139] Mirjalili S, Lewis A. The whale optimization algorithm. *Adv Eng Software* 2016;95:51–67.
- [140] Mirjalili S. SCA: a Sine Cosine Algorithm for solving optimization problems. *Knowl Based Syst* 2016;96:120–33.
- [141] Shashikant, Shaw B. Comparison of SCA-optimized PID and P&O-based MPPT for an off-grid fuel cell system. In: Nayak J, Abraham A, Krishna BM, Chandra Sekhar GT, Das AK, editors. *Soft computing in data analytics*. Singapore: Springer Singapore; 2019. p. 51–8.
- [142] Rashedi E, Nezamabadi-Pour H, Saryazdi S. GSA: a gravitational search algorithm. *Inf Sci* 2009;179:2232–48.
- [143] Sarjila R, Ravi K, Belwin Edward J, Kumar KS, Prasad A. Parameter extraction of solar photovoltaic modules using gravitational search algorithm. *J Elect Comput Eng* 2016;2016:6.
- [144] Yang X-S, Deb S. Cuckoo search via Lévy flights. *Nature & biologically inspired computing, 2009 NaBIC 2009 world congress on: IEEE*. 2009. p. 210–4.
- [145] Das SK, Verma D, Nema S, Nema RK. Shading mitigation techniques: state-of-the-art in photovoltaic applications. *Renew Sustain Energy Rev* 2017;78:369–90.
- [146] Belhachat F, Larbes C. A review of global maximum power point tracking techniques of photovoltaic system under partial shading conditions. *Renew Sustain Energy Rev* 2018;92:513–53.
- [147] Huang Y-P, Chen X, Ye C-E. A hybrid maximum power point tracking approach for photovoltaic systems under partial shading conditions using a modified genetic algorithm and the firefly algorithm. *Int J Photoenergy* 2018;2018:13.
- [148] Daraban S, Petreus D, Morel C. A novel MPPT (maximum power point tracking) algorithm based on a modified genetic algorithm specialized on tracking the global maximum power point in photovoltaic systems affected by partial shading. *Energy* 2014;74:374–88.
- [149] Harrag A, Messalti S. Variable step size modified P&O MPPT algorithm using GA-based hybrid offline/online PID controller. *Renew Sustain Energy Rev* 2015;49:1247–60.
- [150] Rao R. Jaya: a simple and new optimization algorithm for solving constrained and unconstrained optimization problems. *Int J Ind Eng Comput* 2016;7:19–34.